TÉCNICO LISBOA

Role of adenosine A_{2A} Receptors in Multiple Sclerosis: Neural Stem Cells as a potential target

Ana Marta Alonso Gomes

Thesis to obtain the Master of Science degree in

Biomedical Engineering

Supervisors: Prof. Sara Alves Xapelli

and Prof. Maria Margarida Fonseca Rodrigues Diogo

Examination Committee

Chairperson: Prof. Cláudia Alexandra Martins Lobato da Silva

Supervisor: Prof. Sara Alves Xapelli

Members of the Committee: Prof. Adelaide Maria Afonso Fernandes Borralho

November 2018

Acknowledgements

Em primeiro lugar, gostaria de agradecer à Professora Ana Sebastião por me ter acolhido no seu grupo para a realização deste projecto.

Um enorme obrigada à minha orientadora ao longo deste percurso, a Professora Sara Xapelli. Pela forma carinhosa com que fui recebida por si e por todos os membros da sua equipa, desde o início. Agradeço-lhe pelo apoio e disponibilidade total, por todo conhecimento, calma e ponderação que me transmitiu ao longo destes 6 meses. Cresci e aprendi muito e, por isso, terá sempre a minha gratidão.

À Professora Margarida Diogo, agradeço pelo apoio e confiança dados no início deste projecto. Obrigada pela disponibilidade e atenção que sempre demonstrou.

Aos meus queridos colegas e amigos do ASeb Lab e, em particular, ao nicho mais proliferativo e amigável que existe, só me resta agradecer por tornarem esta experiência ainda mais enriquecedora. Dá gosto trabalhar com pessoas assim. Obrigada, Joana, por tudo mesmo. Pela paciência para me ensinares tudo o que eu sei, pelos conselhos sobre tudo e mais alguma coisa e, acima de tudo, por te importares sempre. Não há gelados da Nanarella suficientes que retribuam tudo o que me transmitiste. Obrigada, Diogo, pela tua ajuda essencial nas longas horas de perfusões e por aqueles abraços a que eu nunca sei muito bem como reagir. Obrigada, Rui, por seres esse poço de motivação, com um "fortíssimo!" que chega sempre na hora certa, até porque chega a toda a hora. Um obrigada à Sara Paulo, por toda a ajuda e conselhos durante os *western blots* e por todas as conversas inspiradoras. Obrigada, Filipa, pelas horas passadas nas cirurgias e por teres sempre um sorriso e uma piada pronta para fazer alguém feliz. *Thank you, Marit, for being my one and only "desk" mate.* Ao João Moreira, por ter começado comigo neste novo mundo. Aos "*Mizézes"*, em particular, ao João Gomes, Catarina Beatriz e Sara Tanqueiro, por serem o melhor esquadrão de *western blotting.* Ao Miguel, por ser um companheiro de fins-de-semana de Agosto no laboratório. E aos ratinhos, citando o Diogo, pelo seu "contributo à ciência".

Resta-me também agradecer ao Daniel Costa, do Biotério, pelos conselhos durante a fase pós-cirúrgica dos animais e à Ana Rita Pires, da Histologia, pela ajuda fundamental na preparação das amostras para imunohistoquímica e luxol.

Quanto a MEBiom, ao núcleo duro que tornou Lisboa uma casa e que fez da minha casa um lar. Ao Filipe, à Filipa, às Joanas da minha vida, à Mariana, à Margarida, à Clara, à Bárbara, à Tânia, à Bia, por todas as horas de estudo, de riso, de trabalho, de frustração e de festa. Ao Ricardo e à Joana Moreira. Um obrigada a todos por terem tornado estes 5 anos tão intensos e tão bons. À minha Di, ao meu Tomás e à minha Rosa por serem a minha dispensa transmontana desta casa lisboeta. E à Doina por ser a minha dispensa moldava.

E, por fim, à minha família. À minha irmã por estar tão perto e por ser o meu ponto de referência desde sempre. Ao Miguel, por me falar na Engenharia. E a ambos por me darem a Laura. E, por último, aos meus pais, a quem nunca serei capaz de agradecer o suficiente, até porque eles não permitem que lhes agradeça. Obrigada por tudo o que me proporcionaram e por todo o amor.

Resumo

A Esclerose Múltipla (EM) é uma doença crónica, neuroinflamatória, autoimune e desmielinizante do sistema nervoso central (SNC). A patologia da doença inicia-se com uma resposta inflamatória exacerbada que danifica a bainha de mielina que reveste o axónio. Os oligodendrócitos (OLs), células da glia produtoras de mielina no SNC, provêm da diferenciação de células progenitoras de OLs, existentes no parênquima cerebral, e de células estaminais neuronais provenientes da zona subventricular, um dos nichos neurogénicos do SNC.

O modelo animal de Encefalomielite autoimune experimental (EAE) é dos mais utilizados na investigação da EM. Estudos anteriores observaram um fenómeno espontâneo de remielinização pela migração de OLs para áreas desmielinizadas, também demonstrado em lesões de pacientes com EM. Paralelamente, observou-se uma função neuroprotectora dos receptores de adenosina A_{2A} ($A_{2A}R$) face a condições inflamatórias do modelo de EAE, atenuando o fenótipo da doença.

Deste modo, este projecto pretende analisar o papel dos $A_{2A}R$ no processo de diferenciação de OLs sob condições patogénicas de EAE. Para tal, fêmeas murganhos C57BL/6, foram imunizadas com MOG_{35-55} e injectadas com toxina Pertussis. Seguidamente, foram realizadas cirurgias estereotáxicas para implantar bombas micro-osmóticas que administram no ventrículo lateral a solução do agonista de $A_{2A}R$ (CGS21680, 100 nM) ou o veículo, durante 26 dias.

Realizaram-se testes comportamentais como forma de avaliar a progressão do modelo, em complemento com análises celulares e moleculares de forma a avaliar a desmielinização, inflamação e a activação de OLs. Contudo, a baixa incidência do modelo limitou a relevância dos resultados. Optimizações no protocolo de indução poderão permitir futuras conclusões acerca da aplicação dos $A_{2A}R$ na terapêutica da EM.

Palavras-chave: Esclerose Múltipla, Modelo EAE, Receptores de adenosine A_{2A}, Oligodendrogénese adulta, Remielinização.

Abstract

Multiple Sclerosis (MS) is a chronic neuroinflammatory autoimmune demyelinating disease of the central nervous system (CNS). MS pathogenesis begins with an exacerbated inflammatory response that deteriorates the myelin sheath that insulates neuronal axons. In the CNS, oligodendrocytes (OLGs) are the glial cells that produce the myelin sheath. Myelinating OLGs result from the differentiation of oligodendrocyte progenitor cells (OPCs) present in the brain parenchyma but also from neural stem cells (NSCs) of the subventricular zone (SVZ) neurogenic niche.

Experimental Autoimmune Encephalomyelitis (EAE) is an animal model of MS sorely used in MS research. Previous studies have reported a spontaneous phenomenon of remyelination also seen in MS pathology, through the migration of OLGs to demyelinated areas. Furthermore, adenosine A_{2A} receptors ($A_{2A}R$) have been shown to have a protective role against inflammation in EAE, attenuating the phenotype of the disease. However, $A_{2A}R$ role in modulating adult oligodendrogenesis was not studied.

Thus, the aim of this project is to assess the role of $A_{2A}R$ in promoting OLGs differentiation and myelination under EAE pathogenesis. Female C57BL/6 mice were immunized with MOG_{35-55} and injected with Pertussis toxin to induce the EAE model. EAE mice were administered in the lateral ventricle with vehicle or with $A_{2A}R$ agonist (CGS21680, 100 nM) for 26 days using micro-osmotic pumps.

Behavioural tests were performed to evaluate EAE progression, along with cellular and molecular analyses to assess the role of $A_{2A}R$ agonist on inflammation, OLG differentiation and de- and remyelination. Low incidence of the EAE model limited the relevance of the results. Improvements on EAE induction protocol may allow further conclusions on $A_{2A}R$ relevance for regenerative therapies in MS.

Keywords: Multiple Sclerosis, EAE model, Adenosine A_{2A} Receptors, Adult Oligodendrogenesis, Remyelination.

Table of Contents

List of figures

List of tables

List of Abbreviations

$A_{2A}R$ – Adenosine A_{2A} receptors

aCSF – Artificial cerebrospinal fluid

BBB – Blood brain barrier

BrdU – Bromodeoxyuridine

cAMP – cyclic adenosyl monophosphate

CC – Corpus callosum

CFA – Complete freund's adjuvant

CGS – CGS21680

CNS – Central Nervous System

CREB – cAMP responsive element binding-protein

CS – Clinical score

CTRL – Control

DG – Dentate gyrus

EAE – Experimental autoimmune encephalomyelitis

ERK(1/2) – Extracellular signal-regulated kinases 1/2

GPCRs – G-protein coupled receptors

i.p. – Intraperitoneal

icv – intracerebroventricular

IHC – Immunohistochemistry

LFB – Luxol fast blue

MAPK – Mitogen-activated protein kinase

MBP – Myelin basic protein

MOG_{35-55} – Myelin oligodendrocyte glycoprotein 35-55

MS – Multiple Sclerosis

NF-κB – Nuclear factor κB

NPCs – Neural precursor cells

NSCs – Neural stem cells

OF – Open field

OLGs – Oligodendrocytes

OPCs – Oligodendrocyte precursor cells

p.i. – Post-induction

PBS – Phosphate-buffered saline

PFA – Paraformaldehyde

PKA – Protein kinase A

PLP – Proteolipid protein

PT – Pole test

PTX – Pertussis toxin

RMS – Rostral medial stream

RR – Rotarod

RRMS – Relapsing Remitting Multiple Sclerosis

RT – Room temperature

SCs – Stem cells

SPF – Specific pathogen free

SVZ – Subventricular zone

VAF – Virus antigen free

VEH – Vehicle

WB – Western blot

1. Introduction

1.1. Multiple Sclerosis: Why is it important to understand it better?

Multiple Sclerosis (MS) is a chronic neuroinflammatory autoimmune demyelinating disease of the central nervous system (CNS). MS has been entitled has the most common demyelinating disease of the western world, although with an heterogenous prevalence worldwide[1]. In fact, a recent report elaborated by the Multiple Sclerosis International Federation (MSIF) in 2013 has stated that the estimated number of people with MS increased globally from 2.1 million in 2008 to 2.3 million in 2013, with a female/male ratio of 2:1[2]. The average clinical onset of MS is typically between the ages of 20 to 45, with occasional childhood or late middle age cases[3].

Female-to-male ratio of MS incidence along with the variation of prevalence in different regions of the world is assumed to be associated to some of the aetiologic factors of MS. Although, aetiology of MS is still not fully understood, both genetic and environmental factors are thought to play roles in the development of this illness. For instance, in terms of genetic factors, family recurrence rate is of 20% and genetic mutations in the human leukocyte antigen (HLA) have also been associated with this pathology[4]. In regard to environmental factors, infectious agents such as the Epstein Barr virus (EBV) and the human herpes viruses 6A have been linked to the condition[5]. Moreover, low levels of vitamin D ingestion along with low sun exposition, especially during childhood, have also been associated with a predisposition to develop MS[5]. Nevertheless, further studies and clinical trials are required to assess the actual role of these factors in triggering MS pathogenesis. For instance, in the last decade, many studies have suggested that some epigenetics alterations are a potential risk factor in the development of MS pathophysiology[6]. Yet, stronger evidence is necessary to achieve potential therapeutic targets for MS treatment.

1.1.1. MS pathogenesis and pathophysiology

Although the origin of MS pathology is not yet fully understood, its pathogenic agents and lesions have been thoroughly described and analysed. An exacerbated immune-mediated inflammatory response has been entitled as the main cause of multifocal areas of demyelination and inflammation, commonly known as sclerotic plaques, the pathological hallmark of MS[7]. These lesioned plaques comprise variable levels of oligodendrocyte depletion, myelin degradation, inflammatory mediators, gliosis - proliferation of glial cells, namely, astrocytes, to injured areas of the CNS[8] – and axonal loss[9]. The intense demyelination observed in MS pathogenesis is due to antigen-specific targeting of myelin, mainly disturbing the myelin sheath. The myelin sheath is the insulating layer that insulates the neuronal axon, required for a rapid transduction of action potentials between neurons, thus, contributing to the efficient functioning of the whole neural circuitry mechanisms in the nervous system[10]. Thus, any damage caused to this sheath compromises the efficiency of neuronal communication, triggering many of the symptoms observed in MS pathology. In fact, loss of axonal insulation and the consequent inability

of demyelinated axons to transmit fast impulses leads to sensory or motor neuron failure, which is considered the cause behind MS pathological fatigue[4].

MS characteristic neuroinflammatory environment results from an intensified infiltration of T and B lymphocytes, although the latter in a smaller amount[11], from the blood stream into the CNS, suggesting that MS exacerbated inflammatory response is T cell-mediated. Inflammatory CD4+ and CD8+ T cells, as Th1 and Th17, B cells and antigen-presenting cells (APCs), as macrophages, accumulate in the CNS while secreting pro and anti-inflammatory cytokines that amplify the immune response through the recruitment of microglia[5]. This enhanced migration of inflammatory mediators is dependent of an increase in blood brain barrier (BBB) permeability, initially caused by an adhesion of lymphocytes to the BBB endothelium. Subsequently, the intensified migration of these cells into the CNS parenchyma leads to a BBB disruption, easing the inflammatory process progression[7]. Produced cytokines, as inflammatory interleukins IL-23, IL-21 or the tumour necrosis factor-α (TNF-α), will damage the myelin sheath that coats the axon, causing an incorrect transmission of the action potential and consequently triggering deficient neuronal communication. In addition, B cells produce myelin-specific antibodies which cause further damage to oligodendrocytes (OLGs) – the glial cells responsible for producing this myelin sheath in the CNS – indirectly promoting a breakdown of the myelin sheath and leading to axonal loss[12]. Thus, as demyelination injuries accumulate along with OLGs ablation, the disruption of the myelin sheath will leave the axon vulnerable to degeneration. Hence, accumulation of axonal loss will prompt further neuronal degeneration, causing disease progression[4,13].

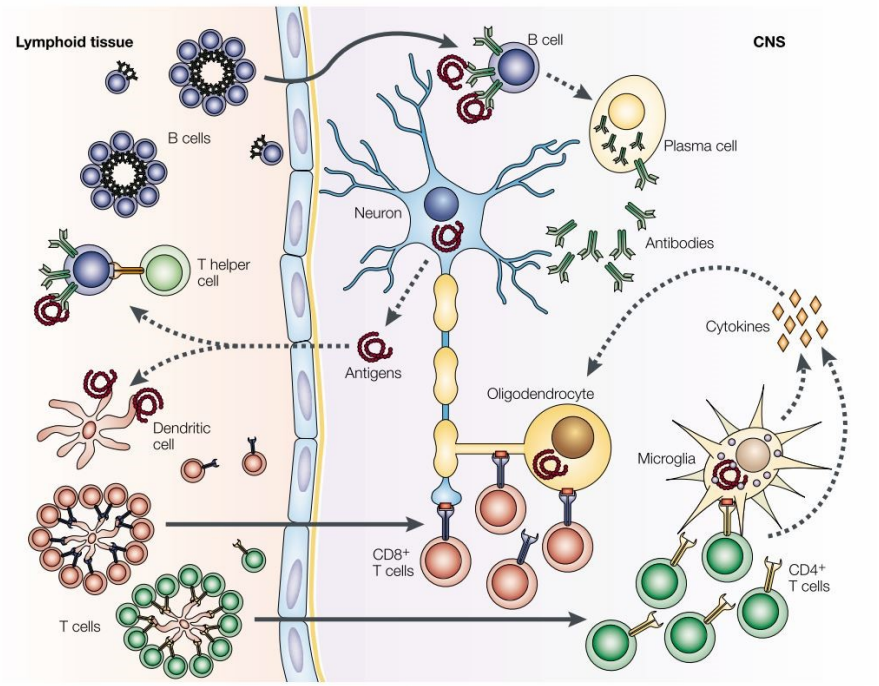

Figure 1. MS immune-mediated inflammatory response. Inflammatory T cells and B cells enter the CNS through the BBB. Inflammatory cytokines production along with microglia recruitment damage oligodendroglial cells, the glial cells that produce the myelin sheath in the CNS, and the myelin sheath itself. Moreover, B cells or plasma cells produce myelin-specific antigens that also participate in the insult against OLGs and myelin. (Adapted from Hemmer et al., 2002[14]).

Yet again, what triggers MS pathogenic mechanisms is still unknown. Most believe that the exacerbated inflammatory response will consequently cause demyelination and tissue damage throughout the CNS. However, it has also been proposed that a neurodegenerative process occurs in the first place, initiating the immune-mediated response[12].

Importantly, many studies have reported a spontaneous myelin repair in MS lesions, as a response to the demyelination phenomenon[15]. The main agents of this endogenous remyelinating response are mature myelinating OLGs, derived from oligodendrocytes precursor cells (OPCs) proliferation and maturation[13]. Prineas et al. have observed in *post-mortem* samples of MS patients, remyelination in lesioned plaques, during ongoing inflammation[16]. However, while this natural process is extremely relevant in early onsets of the disease or in acute lesions, in chronic conditions, as demyelination lesions accumulate and, consequently, disability and pathological impairments occur, remyelination becomes insufficient[17]. In fact, Goldschmidt et al. have observed in brain biopsies samples of MS patients that remyelination events were significantly more intense in early than in chronic MS[18].

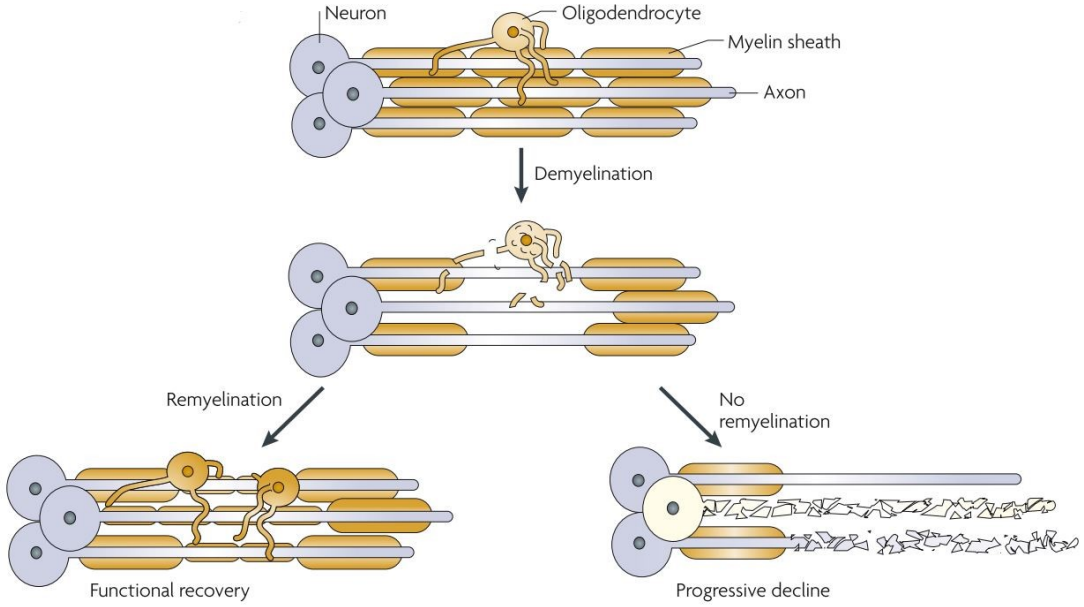

Figure 2. Endogenous remyelinating response to demyelination. At early stages of MS, demyelination can induce an endogenous remyelinating response involving newly formed myelinating OLGs. As demyelinated lesions accumulate, remyelination fails to occur, leading to axonal loss and further disease progression. (Adapted from Franklin et al., 2008[13]).

MS pathophysiology can be expressed in four different forms. Relapsing Remitting MS (RRMS) accounts for approximately 85% of MS cases, being characterized by acute relapses that evolve during days to weeks, followed by partial or full recovery (remitting), with no neurological function deterioration. 80% of people who suffer from RRMS will develop Secondary Progressive MS (SPMS), expressed as initial relapses followed by gradual neurological deterioration associated with acute relapses[2]. A third type of MS, which usually affects 10% of MS patients, is the Primary Progressive MS (PPMS), described as a steady functional decline from the onset of the disease, although with no relapses. And, lastly, known to affect 5% of MS patients is the Progressive Relapsing MS (PRMS), whose phenotype is very similar to the functional declined observed in PPMS although with later acute relapses (Table 1)[5].

Table 1. Types of MS.

Forms of MS	Disease Course
Relapsing Remitting MS	Acute attacks (relapses) that evolve during days to weeks, followed by partial or full recovery (remitting), with no neurological function deterioration.
Secondary Progressive MS	Initial relapses that are followed by gradual neurological deterioration associated with acute attacks.
Primary Progressive MS	Steady functional decline from the onset of the disease with no relapses.
Progressive Relapsing MS	Functional decline from the onset of the disease with later superimposed relapses.

MS patients present a wide range of symptoms and the phenotype varies significantly between patients. The most common symptoms are sensory (40%) and motor (39%), being the least common pain (15%) and cognitive issues (10%)[2]. Specifically, some of these symptoms include vision limitations, weakness, dyscoordination, sensory loss or distortions and fatigue[5].

1.1.2. MS current therapies

Current MS therapies are focused on improving the quality of everyday life by masking individual symptoms, as pain and spasticity – muscular stiffness. For physical recovery, patients are encouraged to perform physiotherapy and, in cases of anxiety or depression, psychological counselling is also advised[19].

The majority of approved medical drugs to treat MS are included in the Disease Modifying Therapies (DMTs) category, to reduce the number and severity of relapses. Some examples of approved DMTs are interferon beta drugs (IFN-Beta), natalizumab, glatiramer acetate or dimethyl fumarate[20]. The mechanism of action of IFN-Beta drugs that promotes the improvement of MS symptoms is still uncertain, although it is probably related to inflammatory effects, by inhibiting inflammatory T cells activation and proliferation, and immune effects, by reducing pro-inflammatory cytokines expression, thus inducing anti-inflammatory cytokines production[5].

Nonetheless, most of these treatments have proved to be more effective in RRMS form, lacking capacity to treat the progressive types of MS. Thus, the main dilemma on the field of MS therapy relies in the risk-benefit ratio of these therapies, and the different roles that these drugs might have on different MS forms[20]. Hence, current MS therapy has been mainly focused on modulating inflammation. However, research is moving forward to develop strategies that will enhance the remyelination response to ameliorate myelin loss and improve axonal protection, thus, delaying disease progression[21]. Therefore, stem cell-based therapies have gained relevance, due to stem cells (SCs) self-renewal and differentiation abilities[22].

1.1.3. Potential of Stem Cell-based Therapies

Cell therapies research in MS therapeutics has been focused on developing effective strategies to delay or ablate progressive neurodegeneration observed in MS. Concurrently, this issue has been tackled mostly through three different cell therapy strategies. The first consists of improving the aberrant immune system response by transplanting autologous haematopoietic stem cells (AHSCs) in order to "reboot" this response; the second strategy is based on the mobilization of endogenous stem cell populations as to explore their neuroprotective capacities; and, lastly, oligodendrocyte replacement by autologous-induced pluripotent stem cells (iPSCs) to supplant the inability of OLGs population to tackle demyelination under MS pathogenesis[23].

AHSCs transplantation therapeutic effect on MS consists of the suppression of the inflammatory activity, an increase in immune tolerance due to the renewal of the immune system response, preventing further disease relapses[23]. However, samples from autopsies of MS patients that received AHSCs transplantation showed lesions of active demyelination and intense inflammation, suggesting that disease progression continued after the AHSCs treatment[24]. Therefore, further comparative trials are required.

It has been observed in experimental autoimmune encephalomyelitis (EAE), a widely used animal model of MS, that the transplantation of neural stem cells (NSCs) or mesenchymal stem cells (MSCs) attenuated neurological dysfunction and enhanced remyelination[25,26]. In fact, Douvaras et al. were able to successfully derive OPCs and mature myelinating OLGs form MS patients iPSCs, and its myelinating capacity has proved effective as demonstrated by *in vivo* myelination using an immunocompromised mouse model[27]. OLGs replacement by reprogrammed iPSCs has been assessed in animal model testing and it has not been transduced to clinical trials yet.

However, iPSCs transplantation has some limitations, with the reprograming protocol being very difficult to reproduce and associated risks of tumour formation due to their genomic instability. Moreover, under MS neuroinflammatory conditions, OLGs and OPCs still exist in great number, the problem remaining in their inability to respond to demyelination. Hence, some believe that SCs transplantation into these hostile conditions may not be the most effective therapeutic method. As proinflammatory cytokines and demyelinated lesions continue to accumulate, the addition of more cells into these hostile conditions might be ineffective, as these mechanisms may also inhibit the regeneration capacity of the newly transplanted cells[21].

Thus, there is a necessity of developing strategies that can in some way resist to or improve this pathogenic environment, by providing support to existing OLGs and enhancing endogenous remyelination.

1.1.4. Potential of endogenous remyelination therapies

Strategies to enhance endogenous remyelination can either follow three ways: removal of factors that inhibit remyelination; promote OPCs proliferation and maturation into myelinating OLGs; enhance OPCs recruitment to demyelinated areas. Drug-screening assays of several compounds, as benztropine and clemastine have been confirmed to enhance remyelination through OLGs instead of immunosuppressive effects[28]. Some of the approaches to enhance remyelination focus on the

modulation of intrinsic signaling pathways that regulate OLGs maturation, myelination or that have a neuroprotective effect under neuroinflammatory environments[28]. For instance, Notch1 or Wnt signaling pathways are known to inhibit OLGs differentiation and, thus, remyelination under demyelinating conditions[29,30]. In turn, MAPK/ERK(1/2) activation has been proved to regulate myelin thickness and timing of OLGs myelination[31]. Moreover, extracellular environment regulation, as clearance of damaged myelin components, for example myelin-associated glycoprotein (MAG), has also been useful to provide greater chances of remyelination[28].

1.1.5. Animal models of Multiple Sclerosis

Animal models that resemble MS pathogenic conditions have been extremely useful in MS therapy research, allowing the assessment of different pathophysiological mechanisms. Many studies on the potential of MS therapeutic approaches were performed using demyelinating and neuroinflammatory animal models. Although these models can reproduce some of the cellular interactions and disturbances in neuroinflammatory and demyelinating conditions observed in MS, none is fully capable of replicating all MS stages. These models can be divided in three major categories: toxin-induced, virus-induced and immune-mediated[32].

Toxin-induced mediated models are characterized by focal demyelination lesions caused by direct injections of gliotoxins, as ethidium bromide, or the systemic administration of cuprizone toxins. Particularly, cuprizone toxin administration is a chemical form of inducing demyelination due to the high toxicity that this compound has against the myelin sheath, also eliciting OLGs dysfunction. It has been described as a high reproducible model, suitable for analysing demyelination and remyelination processes and OLGs apoptosis, although lacking immune response mechanisms, typical of MS pathogenesis[33].

Virus-induced models of MS support the hypothesis that environmental factors, as viral agents, are linked to the initiation of MS pathogenesis. Theiler's murine encephalomyelitis virus (TMEV) is the most used and described model of this category. TMEV infection acts mainly on neurons, leading to axonal damage and consequently activating microglia. The extended and multifocal inflammatory response triggers rapid virus replication in neurons, exacerbating neuronal death and producing of virus-specific pro-inflammatory T and B cells, that will incite axonal demyelination[34]. Nevertheless, although TMEV model is quite approximate to MS pathogenesis, its severity is dependent on mouse strain and gender and its induction is quite demanding and time-consuming[32].

Regarding immune-mediated models of MS, the EAE model is one of the most used animal models in MS research, for sharing many of the clinical and neuropathophysiological features of this condition.

1.1.5.1. Experimental Autoimmune Encephalomyelitis (EAE) model

EAE model induction is based on the principle of inducing an immune response directly against CNS antigens. The model discovery dates to the beginning of the 20th Century, in 1925, when rabbits immunized with human spinal cord homogenates, exhibited spinal cord inflammation and paralysis[35]. EAE induced in rabbits or guinea pigs has been proved to be quite similar to MS, since inflammation is observed in both the brain and spinal cord. Moreover, EAE induction in marmosets allows an analysis of the disease pathogenesis in species phylogenetically very close to humans[36]. However, EAE model is mainly induced in rats and mice. Particularly, C57BL/6 mice have been widely used in the literature due to the abundance of transgenic models[37].

Currently, EAE model can be induced through an active or passive form, although principles are much the same, both dependent on the activation of myelin-specific CD4+ T cells, that are easily capable of crossing the BBB, giving rise to the inflammatory cascade. The passive EAE induction form consists of a transfer into naïve mice of myelin-specific CD4+ T cells isolated from mice EAE-induced[38]. This type of induction has proved to be very useful in understanding the role of myelin-reactive T cells in disease pathogenesis[32]. Active EAE induction form consists of animal immunization with emulsified myelin-related antigens. Commonly used myelin-antigens are proteolipid protein (PLP) and myelin basic protein (MBP), both major components of the myelin sheath, and myelin oligodendrocyte glycoprotein 35-55 (MOG_{35-55}), a minor component of the myelin sheath, but extremely encephalitogenic in many species[39]. MOG_{35-55} has become one of the most used peptides in active EAE induction, due to its high availability and producibility and for the pathological features of its induction closely mirroring the ones observed in human MS[40].

MOG_{35-55} antigen is prepared in an emulsion of Complete Freund's adjuvant (CFA), a mineral oil-based adjuvant that increases the peripheral immune response[32]. CFA is supplemented with *Mycobacterium Tuberculosis (M. Tuberculosis)*, responsible for initiating the innate immune system response[36]. The expansion and differentiation of MOG-specific autoimmune cells is enhanced by a set of pertussis toxin (PTX) injections, which, by increasing BBB permeability, facilitates the entrance of autoimmune T cells into the CNS[41].

EAE active induction mechanisms can be divided into two different stages: an induction phase and an effector phase. The induction phase is initiated by the immunization with the myelin-antigen in CFA which will cause the priming of myelin-specific CD4+ T cells. The induction phase is then followed by the effector phase, in which the activated T cells migrate to the CNS, crossing the BBB. Production of inflammatory chemokines and cytokines induces the migration of peripheral mononuclear phagocytes into the CNS, recruits microglial cells, further exacerbating the inflammatory cascade. The aberrant production of inflammatory cytokines, namely, TNF-α, IL-17, interferon-γ (IFN- γ), along with microglial and phagocytic activity will lead to demyelination, OLGs damage and consequent axonal damage in the CNS, all features of EAE pathogenesis[41,32,42].

EAE models have suffered many modifications so as to replicate specific pathological features of MS. These manipulations are highly influenced by the used antigen emulsion, animal strain, gender and age, being highly sensitive to experimental conditions, namely, animal stress and environment[43]. For

instance, depending on the type of mouse strain and myelin-antigen, EAE course can be either acute, chronic progressive or relapsing remitting. EAE phenotype is expressed as flaccid ascending paralysis, beginning with intense inflammatory infiltrates in the spinal cord lumbar region[41]. Phenotype expression starts with a limp tail, followed by hind and forelimb paralysis, progressively[36].

Normally, C57BL/6 mice MOG_{35-55} induced exhibit a classic chronic EAE clinical course. EAE onset occurs 9 to 14 days after immunization, with peak of disease 3 to 5 days after onset. Partial recovery is seen, but 25% of the induced animals will then show an increase in severity again[36,42–44].

1.2. NSCs and neurogenesis overview

NSCs are multipotent stem cells with the ability to self-renew and capable of differentiating into neurons, astrocytes or oligodendrocytes[45]. Neurogenesis is defined as the process of generating functional neurons from adult neural stem/precursor cells (NPCs). Nowadays, it is known that this process is not exclusive of embryonic and perinatal stages, but it is also seen in the adult mammalian brain[45].

There are two main regions of the brain where NSCs are localized: the subventricular zone (SVZ) of the lateral ventricles and, at a lower magnitude, in the subgranular zone (SGZ) in the dentate gyrus of the hippocampus. In the SVZ, NPCs proliferate and migrate through the rostral medial stream (RMS), to the olfactory bulb, where they differentiate into mature interneurons; in the DG the maturation stages take place in the granular cell layer[46].

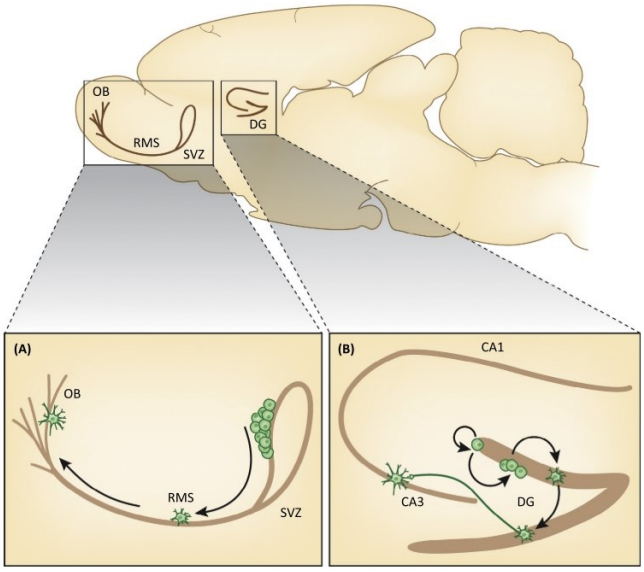

Figure 3. Schematics of the two main neurogenic niches in the rodent brain. A – NPCs migrating from the SVZ in the RMS to the olfactory bulb (OB); **B –** NPCs maturation in the DG. (Adapted from Borsini et al., 2015[46])

The cellular population of these regions has been thoroughly analysed and it has proved to be very enriched and diversified: from endothelial cells, astrocytes, ependymal cells, microglia, mature neurons and progeny of NPCs. Therefore, many of these elements and other molecular cues may have an influence on the fate commitment of these multipotent stem cells. In fact, astrocytes, direct blood-derived cues or microglia were shown to regulate fate specification of adult NPCs as well as neuronal migration, maturation and synaptic formation[47]. Importantly, it has been shown, that under pathological conditions,

differentiation from NSCs can be induced in other CNS regions[48]. In fact, Chang and colleagues have observed in brain samples from MS patients a raise in interneuron density in chronic demyelinated lesions with intense microglia activation. Concomitantly, in demyelinated lesions neighboring the SVZ was also observed an increase of NPCs, suggesting that these lesions produce inflammatory signals that can enhance neurogenesis[49].

1.3. OLGs and oligodendrogenesis overview

Regarding OLGs, the myelinating cells of the CNS, they are the final product of OPCs maturation and differentiation, a mechanism termed oligodendrogenesis. During embryonic development, OPCs derived from SVZ NSCs maturation, migrate and populate the entire brain parenchyma and spinal cord, generating the entire OLGs population that ensures the myelination of the entire CNS during postnatal life[50]. By doing so, OLGs are fundamental glial cells responsible for axonal insulation required for a proper functioning of the nervous system. Any disturbance caused in this myelinating mechanism might be a trigger of neurodegenerative and demyelinating conditions as MS[51].

After postnatal development, OPCs are still found in different structures of the adult brain parenchyma, making 2-9% of the CNS cell population[52]. These remaining OPCs, named adult OPCs, although maintained at a quiescent state of proliferation, are responsible for the maintenance of OLGs and consequent myelin production during adulthood. Adult OPCs density is the most relevant in the hippocampus and neocortex regions[53], with higher density values in white matter than in gray matter, possibly due to higher rates of OPCs proliferation in the white matter[50]. Moreover, evidence has been collected regarding continuous production of OPCs from SVZ-derived NSCs[54] in the adult brain[55]. Ortega et al. have shown that SVZ NSCs produce neurons and OLGs, although the latter in a smaller amount[55]. Additionally, it was also observed a heterogeneous production of OLGs in different SVZ areas, as the dorsal part, that faces the corpus callosum (CC), presents higher levels of OLGs production than the ventrolateral region that faces the striatum[55].

The maturation of OLGs comprises four different stages: OPCs are the precursors with proliferative and migratory abilities, expressing amongst others, Olig2, Sox10 and neuron-glial antigen 2 (NG2); pre-oligodendrocytes are the result of OPC differentiation and start expressing the O4 antigen, while continuing to express Olig2, SOX10 and NG2; pre-myelinating immature oligodendrocytes, start expressing galactocerebroside C (GalC) and stop expressing NG2; myelinating oligodendrocytes express myelin proteins such as MBP and PLP and are fully functional OLGs (fig.4)[10,56].

OLGs production and maturation is highly dependent on extrinsic and intrinsic factors. Regarding extrinsic factors, for instance, in the adult brain, Wnt signaling has been shown to induce OPCs specification in the SVZ dorsal region while bone morphogenic proteins (BMP) has been shown to inhibit OPCs proliferation in the SVZ ventral region[55,57]. Considering intrinsic factors, the transcription factor Olig2 has been proved essential in OLGs differentiation, being induced by Shh signaling and expressed in every stage of OLGs differentiation lineage, from OPCs to myelinating OLGs[53].

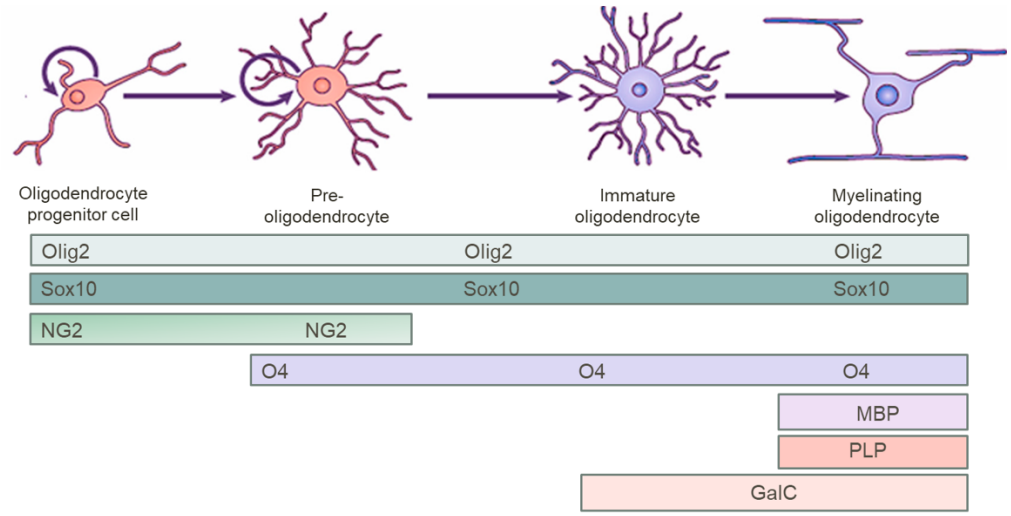

Figure 4. Oligodendrocytic lineage markers. (Adapted from Traiffort et al., 2016[56])

1.3.1. OLGs under neuroinflammatory and demyelinating pathological conditions

Under neuroinflammatory conditions as observed in MS pathology, the exacerbated infiltration of inflammatory mediators and the accumulation of inflammatory cytokines mainly attacks OLGs and myelin, aggravating demyelination.

During early stages of MS, in response to demyelinated lesions, OLGs initiate a spontaneous and robust remyelination process. OLGs derived from OPCs of the brain parenchyma are the main mediators of remyelination[53]. OPCs exit their quiescent form, and initiate proliferation and migration as OPCs are recruited to the lesioned areas. Then, by differentiating into mature myelinating OLGs, these newly-formed cells produce myelin to coat the demyelinated axons. However, parenchymal OPCs have a small migration capacity, being able to just migrate to proximal damaged lesions[53]. Moreover, it has also been observed, that OLGs derived from SVZ OPCs also participate in the remyelination response. This phenomenon was firstly assessed by Menn et al.[54]. In their work, they observed that glial fibrillary acidic protein (GFAP)-positive astrocytes, type B cells, from the SVZ, can generate OPCs that in turn, are able to migrate into the CC, striatum and fimbria where they differentiate into mature myelinating OLGs. Moreover, they observed that, after demyelinating lesions, there was a fourfold increase of OPCs migration into the CC, indicating the participation of SVZ derived cells in myelin repair.

Nonetheless, newly formed myelin sheaths are thinner and shorter and as demyelinating lesions along with intensified neuroinflammation accumulate, myelin repair fails to occur and OLGs loss increases. This inability of OLGs to keep remyelination occurring is mainly due to the release of inflammatory cytokines, the excitotoxic damage and to OLGs high susceptibility to oxidative stress. Therefore, these features turn OLGs more predisposed to cell death in conditions of metabolic stress[50]. Although remyelination occurs in the first place due to inflammatory factors, as IL-1β, or TNF-α, inducing maturation of OPCs into myelinating OLGs[10], myelin debris accumulation inhibits OPCs differentiation[58]. Moreover, in these pathological conditions, activated microglia secretion of excitotoxic factors as glutamate and TNF-α, causes a significant increase in OLGs apoptosis[59], leading to further demyelination.

1.3.2. OLGs therapeutic potential in MS

Many studies have demonstrated the capacity that SVZ-derived OPCs have to migrate to demyelinated lesions and, by differentiating into mature myelinating OLGs, enhance the remyelination response. Picard-Riera et al. have assessed this OPCs and OLGs migration to demyelinated areas in the EAE model[60]. This was the first study to show that the inflammatory and demyelinating pathological conditions of the EAE model induced the differentiation and generation of OLGs, not only in the SVZ but also in the olfactory bulb, which is usually the destiny of neurons originated from the SVZ. This newly formed OLGs migrate from the SVZ to injured CNS areas, especially demyelinated areas such as the CC. In concordance to these findings, Nait-Oumesmar et al. have also observed the mobilization of SVZ-derived OPCs into MS lesions of human *post-mortem* brains[61]. Scolding and colleagues have also observed OPCs presence in chronic and acute lesions of MS patients, although, in comparison, to normal appearing brain regions, there was no significant increase in OPCs density[17]. Nonetheless, given the multifocal nature of MS and the putative minor contribution of the endogenous SVZ cells to remyelination, as compared to the main effectors, the parenchymal OPCs, the efficiency of SVZ cells to promote repair in MS is still relatively modest[51].

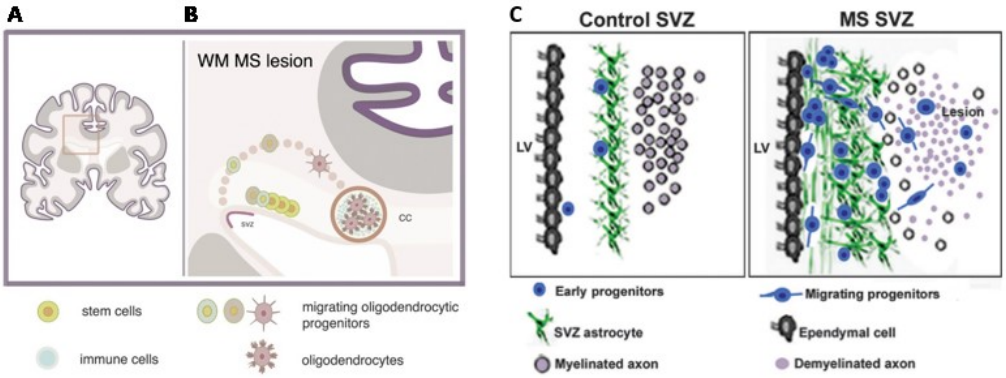

Figure 5. SVZ-derived NPCs activation in response to MS lesions. A – Coronal slice of the brain to localize SVZ and nearby gray matter (GM) and white matter regions (WM); **B –** Migration of NPCs to demyelinated lesions in the CC and maturation of OPCs into myelinating OLGs. (Adapted from Michailidou et al, 2015[15]); **C –** Nait-Oumesmar and colleagues observation of mobilization of SVZ-derived OPCs to MS demyelinated lesions. (Adapted from Nait-Oumesmar et al., 2007[61].

Thus, several research groups have been focusing on finding therapeutic approaches to enhance OPCs proliferation and maturation into myelinating OLGs to support endogenous remyelination[15] and simultaneously provide neuroprotective conditions to these cells. Understanding the mechanisms and signaling pathways that regulate myelin repair, OPCs proliferation and OLGs myelinating action is a promising strategy that can lead to the development of new MS therapeutic techniques. Regarding so, G-protein coupled receptors (GPCRs) have been considered as potential mediators of the neuroinflammatory response. Moreover, their role in OPCs proliferation and differentiation has also been assessed[62].

1.4. Adenosine A_{2A} Receptors

1.4.1. Adenosine role in the CNS

Adenosine is an endogenous purine nucleoside that modulates a wide range of physiological functions, with a relevant influence in cell homeostasis in the CNS. Due to its ubiquitous nature, adenosine can be released by any existing cell, including neurons and glial cells, and its extracellular and intracellular concentration balance makes it an important neuromodulator molecule of the CNS, modulating synaptic plasticity. Also, adenosine has been shown to have a relevant role in sleep and arousal, cognition, memory, neuroprotection and inflammation[63,64].

The mechanisms behind the equilibrium of intra and extracellular adenosine are controlled by equilibrative transporters or nucleoside transporters. Extracellular adenosine can come from the release of ATP, which is broken down by the action of different ectoenzymes, as CD39 and CD73. Intracellularly, this process is controlled by adenosine kinase and 5' -nucleotidase[65]. Hence, the determinant factor in the formation of adenosine is the overall concentration and relative rates of ATP production and catabolism. Nevertheless, there are many factors that can influence the amount of ATP extracellularly, such as cell stress, damage, which will cause membrane integrity loss, leading to an increase of ATP extracellularly, and consequently to an increase of extracellular adenosine. For instance, although extracellular adenosine can be taken up via the above mentioned equilibrative transporters, under inflammatory conditions, this intracellular reuptake is not sufficient.

Regarding adenosine receptors, A_1R, $A_{2A}R$, $A_{2B}R$ and A_3R, these are cell-surface receptors, all belonging to the GPCRs family. A_1R and $A_{2A}R$ are high affinity receptors, which are activated by low levels of extracellular adenosine, whereas $A_{2B}R$ and A_3R are low affinity ones require higher amounts of adenosine in order to be activated[64]. A_1 and A_3 receptors couple to G inhibitory proteins, as G_i or G_O, while A_{2A} and A_{2B} couple to stimulatory G proteins, as G_S. Importantly, Cekik et al. have observed that extracellular accumulation of adenosine, accompanied by activation of adenosine receptors have a relevant role in the regulation of neuroinflammatory conditions as observed in EAE[66].

1.4.2. $A_{2A}R$ role in the CNS

$A_{2A}R$ are expressed in different CNS regions. Particularly, this receptor is highly expressed in striatal neurons, where they usually couple to G_{olf} proteins[67,68]. In addition to the intense expression in the striatum, $A_{2A}R$ is also present in the prefrontal cortex and hippocampus, implying a potential role of this receptor in neuronal development and protection as well as in synaptic transmission[67]. Moreover, $A_{2A}R$ is also expressed in different cell types of the CNS, including OPCs and OLGs, suggesting that these receptors might have a role in modulating neuron and glial communication[69]. Furthermore, Coppi et al. have demonstrated that these adenosine receptors have an effect on OPCs proliferation, migration and maturation into myelinating OLGs[70,71]. Additionally, $A_{2A}R$ are also known for playing a relevant role in the modulation of the immune and inflammatory response[62,67]. Many studies have recognized $A_{2A}R$ as mediators of the anti-inflammatory response, by suppressing pro-inflammatory cytokines expression, leukocyte recruitment and immune cells proliferation. $A_{2A}R$ are expressed in most immune cells, from T

cells, monocytes, macrophages to B cells. These receptors are upregulated during the acute phase of inflammation, limiting the immune response, through protein kinase A (PKA) activation[72].

Nonetheless, in neuroinflammatory conditions, $A_{2A}R$ oppose what is observed in immune cells, with $A_{2A}R$ antagonist shown to attenuate EAE pathology[73].

1.4.3. $A_{2A}R$ role under MS and EAE pathogenic conditions

Dysfunctions in the adenosinergic system have been associated with MS and EAE pathologies. $A_{2A}R$ have been assessed in MS pathology, both in clinical samples and EAE models[74] and they have been recognized as a major mediator of the inflammatory response in EAE model[63], although its role in autoimmune diseases is yet to be completely defined.

Mills et al. have shown the complex and sometimes contradictory role that $A_{2A}R$ have under neuroinflammatory and demyelinating conditions[63]. While using an EAE animal model for multiple sclerosis, they showed that $A_{2A}R$ antagonist treatment protected mice from EAE further development being associated with CNS lymphocyte infiltration. However, $A_{2A}R^{-/-}$ lymphocytes mice developed a more severe acute EAE phenotype characterized by more proinflammatory cytokines and activated microglia. These results confirm the differential role of $A_{2A}R$ signaling on lymphocytes, since it both has anti-inflammatory and promigratory effects on these immune cells. Furthermore, work published and elaborated by Liu et al. has registered that CGS21680, an $A_{2A}R$ agonist, effects on EAE animals were quite protective in terms of disease progression. CGS21680 treatment significantly suppressed lymphocyte proliferation, reduced infiltration of CD4+ lymphocytes, therefore attenuating EAE progression[75].

1.4.4. $A_{2A}R$ participation in NF-κB signaling pathway

One of the most prominent $A_{2A}R$ anti-inflammatory mechanisms is the inhibition of nuclear factor κB (NF-κB) signaling[76]. NF-κB pathway is known to play a role in the modulation of the immune response. Under MS and EAE pathogenesis, NF-κB is activated in many cell types that mediate the inflammatory response, namely, T cells and microglia cells, enhancing inflammatory mediators' production, thus exacerbating inflammation[77]. $A_{2A}R$ have been shown to inhibit this pathway in a PKA-dependent manner, hence suggesting a potential therapeutic role of $A_{2A}R$ in neuroinflammatory MS or EAE pathogenesis[78].

NF-κB is a ubiquitous hetero or homodimer transcription factor highly expressed in many different cell types as T cells, neurons, and glial cells, namely, microglia, astrocytes and oligodendrocytes[77]. NF-κB entitles the NF-κB/Rel family of five transcription factors: p50, p52, p65 (RelA), c-Rel, and RELB. Normally found in its inactivated form in the cytoplasm due to the binding of κB inhibitors (IκB), usually, IκBα. When translocated into the nucleus, NF-κB regulates the expression of a large number of inflammatory genes[79].

The canonical NF-κB signaling pathway can be induced in response to inflammatory cytokines, as TNF-α and interleukin 1 (IL-1), pro-inflammatory cytokines typical in chronic neuroinflammatory diseases as MS. These cytokines are able to stimulate cell-surface receptors, as IL-1 Receptors or Toll-like receptors (TLRs), which will activate the IκB kinase (IKK) complex[80]. Subsequently, this kinase will phosphorylate IκBα leading to its proteasomal degradation. The degradation of IκBα from NF-κB

heterodimers, as p65, allows the translocation of this factor to the nucleus, which is further activated by post-translational modifications as phosphorylation, activating downstream gene transcription[77].

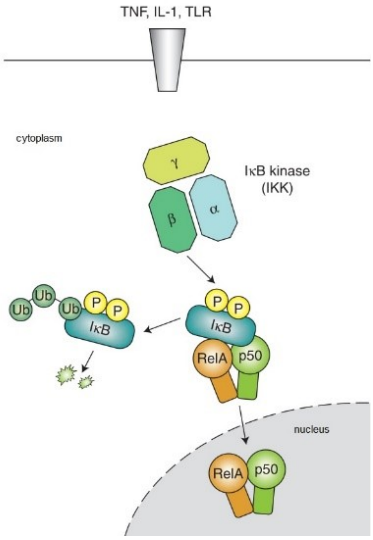

Figure 6. NF-κB signaling cascade. (Adapted from Lawrence, 2009[80])

The influence of the activation of NF-κB in the inflammatory response is mainly due to its participation in pro-inflammatory genes expression, consequently leading to the production of both pro and anti-inflammatory cytokines and chemokines. However, the balance of this ambivalent production leads to an incomplete understanding of NF-κB role in inflammation, which can either be neuroinflammatory protective or enhance the inflammatory response[80].

Nevertheless, NF-κB activation surpasses the regulation of pro and anti-inflammatory mechanisms, by influencing cell differentiation, survival and proliferation. Moreover, particularly in the CNS, NF-κB under neuroinflammatory conditions has been shown to be involved in synaptic, neuroprotection, as well as neural stem cell proliferation and differentiation[81–83]. In fact, Zhang et al. have observed that NF-κB signaling activation functions as an initiator for the NSCs differentiation at early stages of neurogenesis, starting NSCs asymmetric division and further differentiation[83].

$A_{2A}R$ role in NF-κB pathway is essentially inhibitory. $A_{2A}R$ activation by binding of a G_s protein, leads to the activation of adenylyl cyclase (AC) increasing levels of cyclic adenosyl monophosphate (cAMP), an important regulator of immune and inflammatory responses. Subsequently, cAMP signaling causes the activation of cAMP- PKA which, in turn, will activate the nuclear substrate cAMP responsive element binding-protein (CREB). This CREB phosphorylation increase will directly compete with NF-κB, since it also regulates many inflammatory genes, inhibiting NF-κB activation, thus, decreasing pro-inflammatory cytokines expression[67,78]. Hence, $A_{2A}R$ signaling will suppress inflammation in a PKA/CREB-dependent manner.

1.4.5. $A_{2A}R$ role in MAPK/ERK(1/2) signaling pathway

$A_{2A}R$ activate the mitogen-activated protein kinases/extracellular signal-regulated kinases (MAPK/ERK), which primarily influences mitogenesis, differentiation and cell survival. Under EAE pathogenesis, this pathway has been shown to regulate immune cell function, with its inhibition having a minor impact on EAE clinical course[84].

MAPK families' cascades are known for participating in a broad number of complex cellular programs, through the transduction of extracellular signals to cellular responses[85]. This cascade can be divided into a three-step occasion, starting with a MAPK kinase kinase (MAPKKK), followed by a MAPK kinase (MAPKK), ending with a MAPK. These phenomena occur in all types of cells of the mammalian system, taking part, in cell differentiation, proliferation and differentiation, metabolism and apoptosis, through gene expression regulation[86].

One of the many MAPK cascades profoundly described in the literature includes the conventional MAPK/ERK 1/2 family. This signaling pathway is usually activated by extracellular growth factors, cytokines and cell-surface G-protein coupled receptors (GPCRs), as the described adenosine $A_{2A}R$[78]. ERK1/2 is usually present in the cytoplasm but as the signaling cascade develops it can be translocated into the nucleus and, in its activated, form phosphorylate different transcription factors and proteins. In doing so, ERK1/2 plays a major role in cell growth, differentiation and proliferation[85–87].

Likewise, cross-talks between different MAPK families may occur, which can be defining in cell fate mechanisms. For instance, ERK activation of the MAPK c-Jun terminal kinase (JNK) plays a fundamental role in the ERK1/2 capacity of regulating cell differentiation[88]. Moreover, $A_{2A}R$ has been attributed a protective effect in spinal cord injury (SCI) pathology associated with the deactivation of the JNK/MAPK pathway in OLGs[89].

$A_{2A}Rs$ most commonly bind to G_s proteins, activating the enzyme AC. AC activation leads to the production of cAMP which, in turn, will activate cAMP-dependent PKA. In sequence, PKA will trigger the activation of the MAPK/ERK1/2 signaling pathway, although the activation of this kinase cascade may also occur in a PKA-independent manner[78,90].

Recent studies have described that the activation of ERK1/2 pathway is a key intervener of the extracellular signal transduction that regulates oligodendrocyte lineage and development. In fact, Fyffe-Maricich et al. have described that ERK1/2 signaling is activated in OPCs as they differentiate into mature myelinating OLGs[31,91]. Although ERK1/2 absence does not significantly affect OPCs proliferation and differentiation, it disturbs differentiated OLGs capacity of producing myelin sheath. Mutant OLGs, lacking ERK1/2 signaling, were not capable of transcribing essential myelin genes, which led to a poor production of myelin[31]. This data suggests that ERK1/2 activation plays a major role in the myelinating capacity of mature OLGs, supporting myelin thickness formation in the CNS, fundamental for rapid and efficient neuronal communication. Concomitantly, ERK1/2 role in the enhancement of myelination may also be clinically relevant in demyelinating conditions as MS, since it can be a targeted mechanism for improving remyelination of lesioned areas.

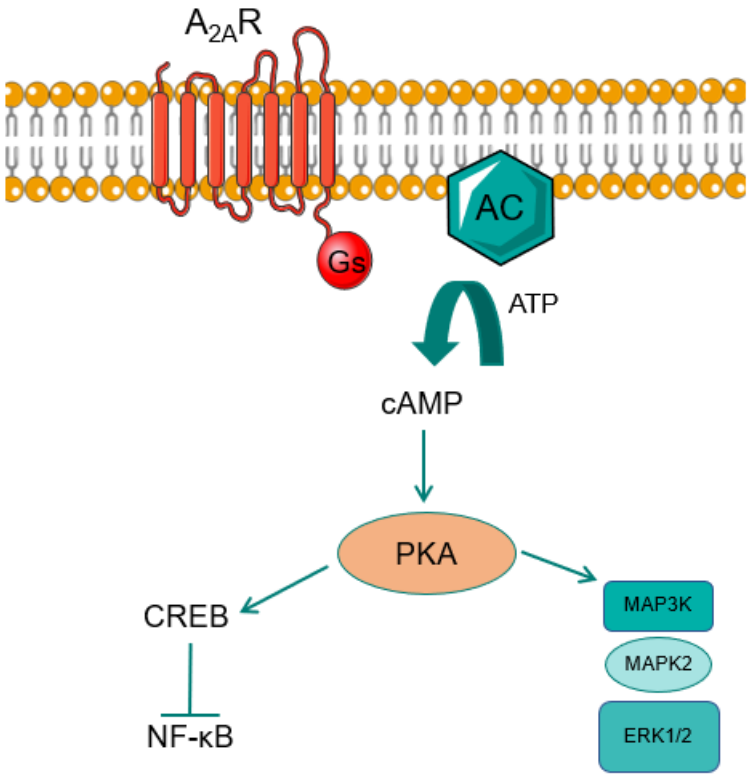

Figure 7. $A_{2A}R$ signaling pathways, regarding NF-κB inhibition and ERK1/2 activation. $A_{2A}R$ activation by binding of a Gs protein, activates adenylyl cyclase (AC) increasing levels of cyclic adenosyl monophosphate (cAMP). Subsequently, cAMP signaling causes the activation of cAMP-PKA which, in turn, will activate the nuclear substrate CREB, directly competing with and inhibiting NF-κB expression, thus, hindering inflammation. In the same PKA-dependent manner, $A_{2A}R$ activation will trigger the activation of the MAPK/ERK1/2 signaling pathway. (Adapted from Morello et al., 2009[78]).

1.5. Aims and Motivation

MS therapeutic and pathophysiological research has become one of the most explored themes in the field of neurodegenerative diseases. Over the years, therapies have been developed, diagnostic techniques have been improved, etiology of the disease and risk factors have been discussed. However, current therapies are only prophylactic and have not yet been able to tackle MS evolution, particularly in its progressive forms. Moreover, the prevalence of the disease worldwide continues to be quite significant[2].

Hence, MS research is now more relevant than ever with OLGs being considered as potential therapeutic targets, due to their ability to spontaneously remyelinate lesioned areas, at early stages of MS. Furthermore, many studies considered stem cells therapies as a great candidate to lead MS treatment forward. However, not much is known on how NSCs maturation into OPCs and the subsequent differentiation into myelinating OLGs occur under MS demyelinating and neuroinflammatory conditions.

Adenosine is known to have a relevant influence in cell homeostasis in the CNS. Its high-affinity A_{2A} receptor is highly expressed in different regions of the CNS as well as in OPCs and OLGs. Moreover, recent studies have shown that A_{2A} receptor has a critical role in the regulation of neuroinflammatory patterns, under MS and EAE pathological conditions, along with its active participation in pathways that regulate cell differentiation and survival. Nonetheless, work performed in our group has assessed that A_{2A}Rs activation in SVZ neurospheres promoted oligodendrocyte differentiation and it also led to an increase of CNPase activity, an enzyme expressed by mature oligodendrocytes, which implies that differentiated OLGs were myelin producers[92].

Thus, in this experimental project I aimed at understanding the role of adenosine A_{2A} receptors in promoting OLGs differentiation and myelination under MS conditions, using the EAE mouse model. In fact, we focused on whether the activation of these receptors could promote an improvement of the EAE model phenotype, by enhancing OLGs myelinating ability. To do so, we proposed to: firstly, induce the EAE model in female C57BL/6 mice; secondly**,** administer intracerebroventricularly A_{2A}R agonist in EAE mice for 26 days; thirdly, assess EAE progression by EAE clinical score follow-up and behavioural performance analysis; and, lastly, perform molecular and cellular analysis to assess A_{2A}R agonist influence in myelination, inflammation and OLGs myelinating capacity.

2. Materials and Methods

2.1. Ethical Concerns

All experimental procedures performed in animals in the following study were carried out always ensuring humane care and minimum animal distress, in conformity with the European Community legislation (86/609/EEC; Directive 2010/63/EU, 2012/707/EU). These procedures were approved by the Animal Ethics Committee of *Instituto de Medicina Molecular* (iMM), as well as by the Direção Geral de Alimentação e Veterinária (DGAV), the Portuguese competent authority for animal protection.

2.2. Animals and Housing

Fifteen young C57BL/6 female mice (ten-weeks old) from Charles River (Barcelona, Spain) were used.

Prior to any *in vivo* procedure, animals were housed in groups of five in individually ventilated cages (IVC) in the iMM rodent facility, in specific pathogen free (SPF) environmental conditions, with an average room temperature of 22ºC and a regular 12h/14h light cycle. Moreover, food and water were provided *ad libitum* and cage environment was enriched with cob bedding. Cage bedding was changed to a softer paper bedding type, after EAE model induction, to provide a more comfortable environment adequate to the disease onset development.

All procedures were performed in SPF conditions. Following micro-osmotic pump surgery implantation, animals were housed individually to avoid unnecessary post-surgical complications, easing recovery. Seven days following EAE induction, animals were moved to a virus antigen free (VAF) area.

Animals were divided in groups of 5 animals: 1) control, a naïve control group that did not go through any experimental procedure; 2) EAE VEH, EAE mice with micro-osmotic pump filled with the vehicle solution, artificial cerebrospinal fluid (aCSF); 3) EAE CGS, EAE mice with micro-osmotic pump filled with the A2A receptor agonist, CGS21680, in aCSF.

2.3. Timeline for *in vivo* experimental procedures

In the first 2 days animals were induced with the EAE disease model. On day 2 post-induction (p.i.), bromodeoxyuridine (BrdU) was administered to label SVZ cell-derived cells. Subsequently, on day 3 p.i., micro-osmotic pump intracerebroventricular (icv) implantation surgery was performed in EAE mice. After the surgery procedure, animals were observed daily in order to assess post-surgical recovery and, starting on day 7 p.i., clinical scores were registered daily, along with weight variations, registered weekly. Parallel to this, handling of the animals was performed between day 7 and day 14 p.i.. Behavioural tests were performed from day 14 to day 25 p.i..

Animals that developed EAE clinical score (CS) were sacrificed at the peak of the disease (day 23 p.i.). The remaining animals were kept until the end of the experiment, to assess possible fluctuations on the disease onset, and were ultimately sacrificed on day 28 p.i.. Brain was removed for posterior

cellular and molecular analysis, namely, western blot assays, immunohistochemistry, and Luxol fast blue staining.

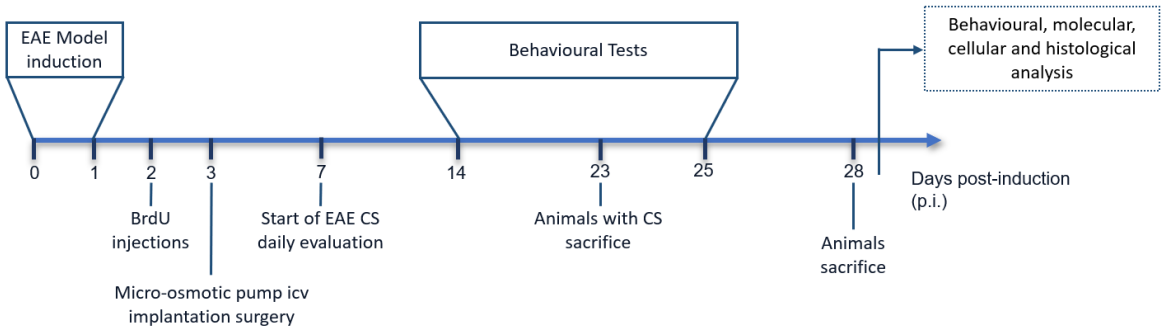

Figure 8. Timeline for *in vivo* experiments.

2.4. EAE Model induction

EAE was induced in mice using a kit (Hooke Kit™ MOG_{35-55}/CFA Emulsion PTX, Cat #EK-2110, Lot #0126)**,** from Hooke Laboratories (Lawrence, MA, USA), according to manufacturer's instructions. This set is composed of an antigen MOG_{35-55} rat emulsion in CFA with mouse heat killed *M. Tuberculosis* and PTX in glycerol buffer.

On day 0 p.i., 100µg of MOG_{35-55}/CFA emulsion were subcutaneously injected in both right and left side of the mouse's ventral flank, making a total of 200µg of injected emulsion. A solution of PTX in phosphate-buffered saline (PBS) (NaCl 137mM, KCl 2.1mM, KH_2PO_4 1.8mM and $Na_2HPO_4.2H_2O$ 10mM, pH 7.4) was prepared fresh and, approximately two hours after MOG emulsion injection, 100µL of PTX (120ng dose per animal[44]), was intraperitoneally injected in the mice right flank. Approximately 24 hours later, on day 1 p.i., a second PTX intraperitoneal (i.p.) injection was administered.

2.5. BrdU Administration

BrdU (5-bromo-2'-deoxyuridine) is a halopyrimidine, an artificial thymidine analogue that can be incorporated in the DNA of dividing cells during the S-phase of the cell cycle[93], thus allowing the labelling of proliferating cells, through immunohistochemistry assays by using anti-BrdU antibodies[94]. Therefore, in order to assess NSCs proliferation and differentiation under EAE conditions, it was performed a BrdU administration protocol to identify SVZ-derived cells, ensuring that any labelled cells in other brain structures are originated from either the SVZ or the RMS[60]. On day 2 p.i., BrdU (Sigma-Aldrich, MO, USA), dissolved in sterile 0.9% NaCl saline solution, was administered i.p. 7 times with 2 hours intervals (50mg of BrdU per Kg of mouse body weight).

2.6. Micro-osmotic pump intracerebroventricular implantation surgery

To study the role of $A_{2A}R$ in oligodendrogenesis in the EAE mouse model, mice were implanted with micro-osmotic pumps containing a solution of the A_{2A} receptor selective agonist CGS21680 (2-(4-(2-Carboxyethyl)phenethylamino)-5'-N-ethylcarboxamidoadenosine, Tocris, Bristol, UK), a monocarboxylic

acid and a dicarboxylic acid monoamine, derived from adenosine[95], in aCSF (NaCl 150mM, KCl 3mM, $CaCl_2$ 1.3mM, $MgCl_2$ 0.8mM, Na_2HPO_4 0.8mM and NaH_2PO_4 0.2mM).

On day 3 p.i, micro-osmotic pump icv implantation surgery (Alzet® Micro-osmotic pump Model 1004 combined with the Alzet® Brain Infusion Kit 3 1-3mm, DURECT Corporation, Cupertino, CA, USA) was performed to the EAE-induced animals.

The micro-osmotic pump mechanism is based on an osmotic pressure difference between a pump compartment, the osmotic pump layer, and the body tissue surrounding the apparatus[96]. The water influx into the osmotic pump layer, causes the displacement of the test solution from the pump at a controlled, predetermined rate, which in this model corresponds to 0.11µL/h[97], with an autonomy of 28-days.

Pumps were prefilled with the aCSF or CGS21680 in aCSF (100 nM) and the prefilled pumps were primed by being placed in sterile saline solution 0.9% NaCl in the incubator at 37ºC, for 48h prior implantation.

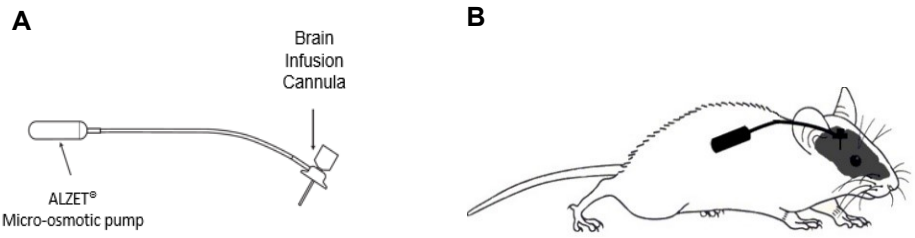

Figure 9. A – Diagram of the Alzet Micro-osmotic pump Model 1004 combined with a Brain Infusion Kit 3 1-3mm; **B –** Schematics of the system implanted in a female C57BL/6. Pump reservoir in the dorso of the mouse and icv implantation of the cannula.

Surgery was performed in the iMM rodent facility surgery room, in a SPF environment. The animal was anaesthetized, with isofluorane (Zoetis, NJ, USA) through inhalation, and kept under a deep anaesthesia stage throughout the whole procedure. To avoid hypothermia, the body temperature was maintained using heating pads at approximately 37ºC. The analgesic Buprenorphine (0.016 mg/ml, in NaCl) was administered subcutaneously (100 µl of analgesic per 15-30g of mouse body weight).

Assisted by a stereotaxic apparatus (Stoelting, IL, USA), the desired coordinates for the icv cannula implantation, were marked in the cranium of the animal. Coordinates were referenced from the bregma point: -0.5mm anterior-posterior (AP), +1mm medial-lateral (ML) and +3mm dorsal-ventral (DV). A small hole was drilled in this position to place the cannula's tube and a subcutaneous pouch was formed to place the pump in the dorsal flank of the mouse. To cannula was sealed in the cranium with acrylic resin (Tab 2000™, Kerr, Upplands Väsby, Sweden). As the implantation procedure was finished, the skin of the mouse was sutured with Silkam® 4/0 silk sutures (Braun, Melsungen, Germany), and Bepanthene® Plus (Bayer, Leverkusen, Germany) was applied on top of the sutures. This system locally administers in the lateral ventricle the CGS21680 in aCSF solution or the vehicle.

Regarding the control group, animals were not submitted to the surgery procedure, but were also housed individually, so social interaction conditions would be the same between experimental groups.

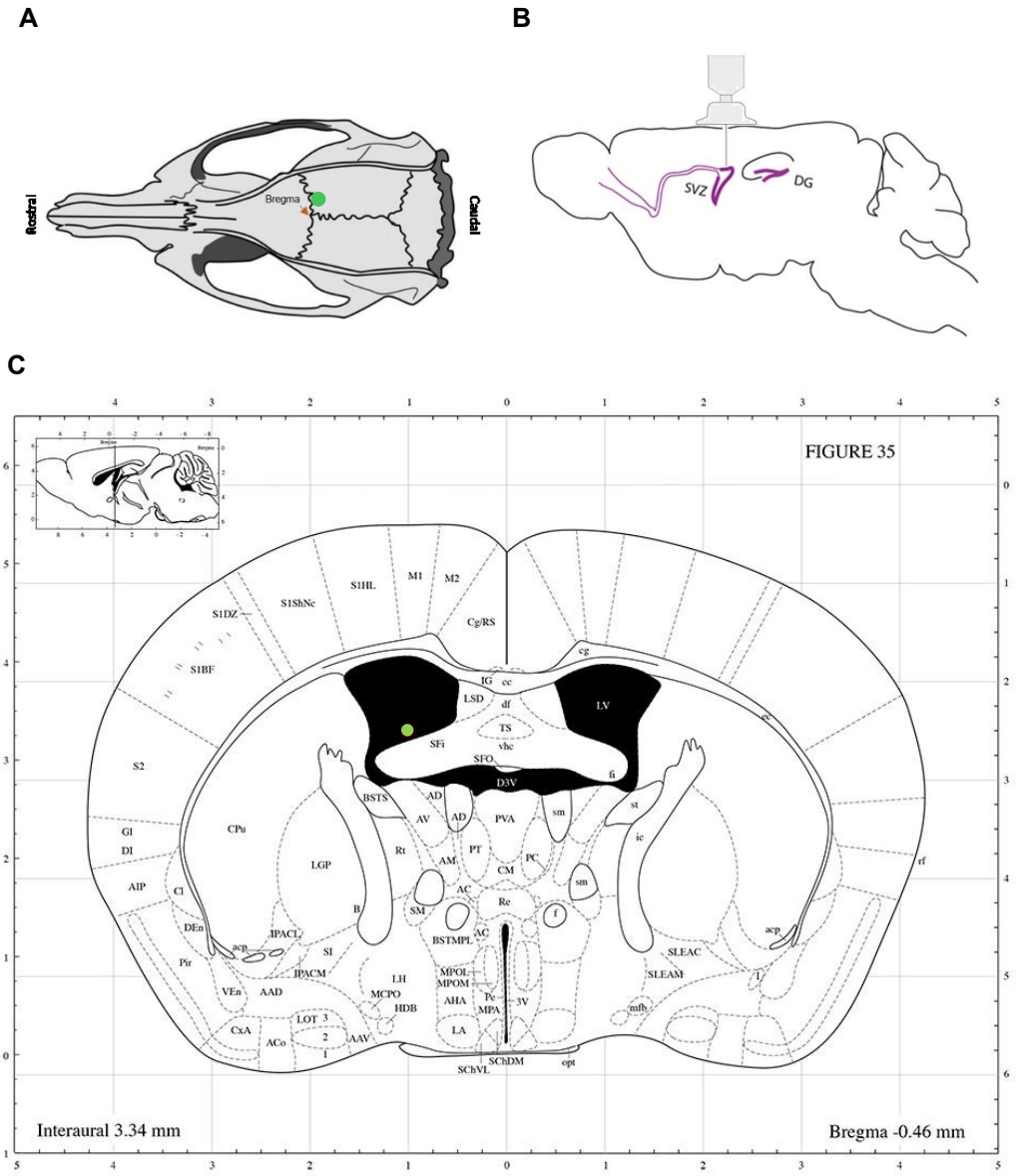

Figure 10. Schematic representation of the brain coordinates for the icv brain infusion cannula implantation. **A -** Top view of the cannula implantation spot (in green), with the bregma point as reference. Coordinates: -0.5mm anterior-posterior (AP), +1mm medial-lateral (ML) and +3mm dorsal-ventral (DV). **B -** Saggital view of the cannula implantation in the lateral ventricle region. SVZ – Subventricular Zone; DG – Dentate Gyrus. **C -** Coronal plan of the cannula location (in green) in the right lateral ventricle of the mouse's brain (Adapted from Paxinos and Franklin, 2004[98]).

2.7. EAE Clinical Score

EAE severity and disease onset was daily evaluated, starting on day 7 p.i., using the following clinical scoring scale: 0, healthy; 1, limp tail; 2, partial paralysis of the hind limbs; 3, complete paralysis of the hind limbs; 4, hind-limb paralysis and forelimb weakness; 5, moribund or deceased[44,99].

2.8. Behavioural Analysis

The first and most visible signs of EAE development in mice are locomotor impairments, displayed as an ascending flaccid paralysis[36]. Three different behavioural tests were performed to complement the CS analysis: pole test (PT), rotarod (RR) and open field (OF). The PT and RR were used to assess motor balance and coordination[100], while the OF test was used to observe general motor activity and exploratory behaviour[101]. This battery of behavioural tests allowed a thorough comparison of EAE progression in both EAE experimental groups, as well as a comparison between control animals. Immediately prior to behavioural tests initiation, handling of the animals was performed for 5 days followed by a two-days interruption to minimize variations in experimental parameters and animal stress during the protocol. Additionally, tests were performed in a controlled environment, with regulated temperature, minimum noise and appropriate lighting. Between different individual tests, set-ups were cleaned with a 30% ethanol solution, to remove olfactory cues. On the first day of each test, animals had a habituation period of 30 minutes to the behaviour room.

Behaviour tests were performed for 2 weeks being initiated on day 14 p.i.. The tests were grouped in two days to reduce physical fatigue. On the first day, PT and RR were performed and on the following day, OF. On the third day, no tests were performed, and then again, the two days of behavioural tests were repeated. Then, there were a two-days pause, and then again the behavioural assessment was repeated.

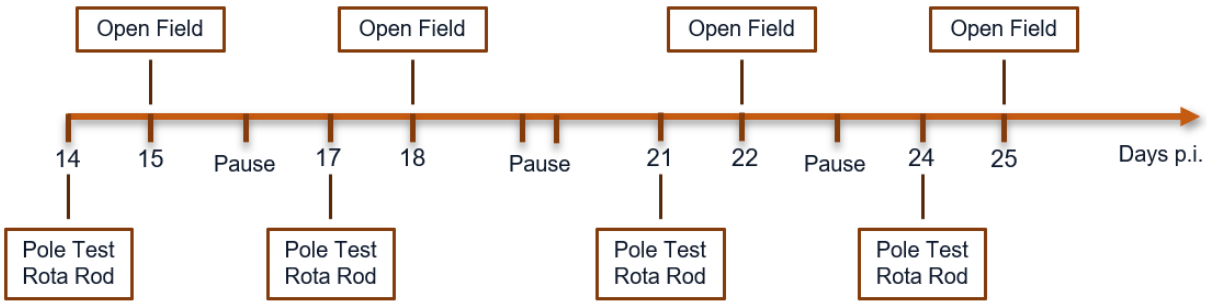

Figure 11. Timeline for behavioural tests.

2.8.1. Pole Test (PT)

PT was performed as previously described, with some minor alterations[100,102]. This test allows an evaluation of locomotor coordination with previous literature describing that the physical requirements demanded by this task are related with neuronal striatal activity[102]. Therefore, since the striatum is a highly demyelinated area during EAE pathogenesis[103] performing this test will allow an indirect assessment of this area.

The protocol was performed under red light and four trials were performed per day, with a minimum 15 minutes interval between each, with the experimenter in the room during the whole protocol. The system entailed a square base (15×15×1.5cm) with a rough-surfaced pole (height 50cm; diameter 2cm) on top of it. The apparatus was placed on a table covered with paper bedding material and paper rolls, so the mouse was more prone to descend the pole. On the first day of PT, at the beginning of the first trial, the animal was set on the table for approximately one minute to freely explore the system, so it

would get familiar with it. The pole was then positioned horizontally, and the mouse placed head-upward on its top. Immediately after, the pole was smoothly placed vertically, and the trial was concluded as the mouse descended the pole and touched the base with its four paws. Trials were excluded when the animal would go up the top of the pole.

The entire task was video-recorded to allow a posterior blind analysis of physical performance parameters. Experimental time began as the animal hind and fore limbs were in contact with the pole. The time the animal took to orient downwards in a 180º movement, $t_{orient,}$ in seconds (s); the time it took for the animal to reach the base of the pole, $t_{descend}$ (s); and total experiment time (t_{total}), which was the sum of both t_{orient} and $t_{descend}$, were registered. In some performances, due to high EAE CS, the animal descended the pole in a lateral body position. In this case, t_{total} is attributed to t_{orient} and, thus, to $t_{descend}$ ($t_{total} = t_{orient} = t_{descend}$)[100]. Nonetheless, if the animal immediately fell off the pole at the beginning of the task, t_{total} is attributed to the highest t_{total} of that group in that trial, as well as t_{orient} and $t_{descend}$ [100]. An average of the four trials is accounted for all parameters.

2.8.2. Rotarod (RR)

The RR test was performed with a minimum 2 hours interval after PT trials were finished. The physical performance demanded by this task allows an evaluation of the motor balance, coordination and fatigue of the animal[104], which can be juxtaposed with the EAE phenotype course over time, as previously described[105].

This test was performed under dim yellow light and 3 trials were performed per day, with a minimum 30 minutes interval between them with the experimenter in the behaviour room throughout the entire protocol. The RR apparatus (Panlab, Harvard Apparatus, Barcelona, Spain) consists of a cylinder with 5 divisions, in which 5 different animals can stand there simultaneously. The system has an acceleration program, which linearly increases velocity from 4rpm to 40rpm, in approximately 300s.

On the first day of RR trials, animals were placed on the rod, for about 2.30 minutes at a constant rotation of 7rpm, as a habituation period to the system. Every time a mouse fell, it was placed on the rod again until the animal was able to stay on the rod without falling. Afterwards, the system was programmed to the accelerating protocol. If the mouse fell before or at 7rpm, it would be placed back on the rod. At the end of each trial, time of fall, t_{fall} (s), and maximum rotation (rpm) reached are registered for every animal. An average of 3 trials is accounted for both parameters.

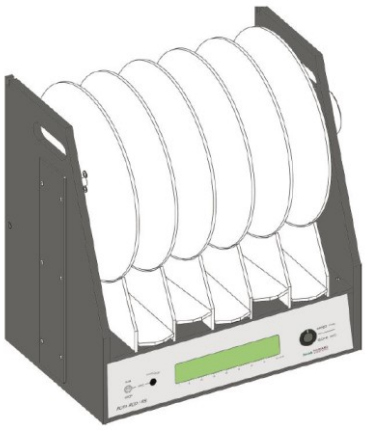

Figure 12. Panlab, Harvard Rotarod apparatus for 5 mice.

2.8.3. Open Field (OF)

OF trial was performed under dim yellow light, the day after PT and RR tasks. The task consisted of placing the mouse in the center of a square wood arena (40×40×40cm). allowing the animal to freely explore it for 10 minutes. This task not only permits another evaluation of the animal locomotor activity and exploratory behaviour, but it also complements EAE scoring as another parameter to assess disease progression. In fact, it has been previously reported that the travelled distance parameter functions as an accurate marker of motor dysfunction in the EAE mouse model[106].

One trial was performed per day under dim yellow light, and the experimenter left the room as the animal was placed in the open field arena. Trials were video-recorded with a camera placed above the arena and were then analysed using the video tracking software Any-maze (Stoelting, Dublin, Ireland). The locomotor and exploratory behaviour of the animals were registered as travelled distance (m) and number of crossings from the peripheral area to the intermediate area and to the central area of the field. Results from different behavioural test days were compared to assess EAE progression.

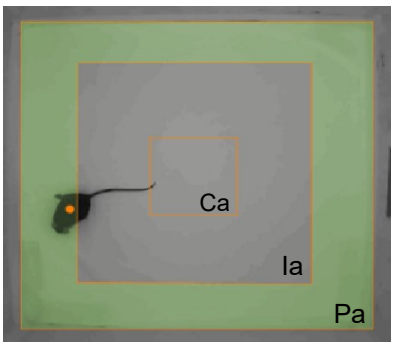

Figure 13. OF test analysis. Areas delimited by the Any-maze software and animal tracking. Ca – central area; Ia – Intermediate area; Pa – Peripheral area.

2.9. Animal Sacrifice and Tissue Processing

EAE induced animals that presented CS above 1 were sacrificed at the peak, on day 23 p.i, two days before behavioural tests were finished. The remaining animals were kept until the end of the protocol, on day 28 p.i.. Animals were deeply anesthetized with isoflurane, through inhalation and transcardially perfused with PBS. Whole animal cardiac perfusion allows the clearing of the circulatory system, since the mouse is in a deep anesthesia state and the natural heart pumping allows the circulation of the clearing buffer.

Afterwards, brain left hemispheres were removed and preserved for tissue post-fixation in 4% paraformaldehyde (PFA) in PBS (pH 7.2) at 4ºC, for 72 hours for immunohistochemistry analysis and Luxol fast blue staining. Subsequently, samples were transferred to an increasing sucrose gradient (15%, 30% sucrose) in PBS at 4ºC to cryoprotect the tissue. Brain right hemispheres were cryopreserved at -80ºC after isolation of the brain areas of interest (SVZ, CC, striatum and cortex) for molecular analysis by western blotting.

For immunohistochemical and Luxol fast blue analysis, left hemispheres were gelatine-embedded and coronally sectioned in 40µm-thick slices between the coordinates +1.5mm and -1.5mm, with bregma as the reference point, using a cryostat Leica CM3050 S (Leica Biosystems, Wetzlar, Germany). Sections were collected in series of ten each serie being an anterior-posterior reconstruction of the SVZ and CC regions and separated by 400µm. Sections for immunohistochemical assays were placed in 24-well plates in anti-freezing medium (30% glycerol, 30% ethylene glycol, phosphate buffer 0.1 M (8.9% $Na_2HPO_4.2H_2O$, 7.8% $NaH_2PO_4.2H_2O$, pH 7.3-7.4) and stored at -20ºC. Sections for Luxol fast blue assays were mounted in microscope slides (Superfrost™ Plus, ThermoFisher Scientific, MA, USA) and stored at -20ºC.

2.10. Cellular and Molecular Analysis

2.10.1. Western Blot (WB)

Samples from SVZ, CC, striatum and cortex were isolated from mice left hemispheres to quantify myelin proteins, as MBP and PLP, by WB assays. Moreover, to assess $A_{2A}R$ signaling pathways activation, Nf-κB phosphorylated and total forms, along with its inhibitor IκBα forms and MAPK/ERK1/2 proteins were also quantified.

Brain tissue samples from these, were homogenized under sonication with Radio Immuno Precipitation Assay (RIPA) lysis buffer (4% Nonidet® P40 Substitute (NP40), 1 mM ethylenediamine tetraacetic acid (EDTA), 150 mM NaCl, 50 mM Tris base), containing a cOmplete™ Mini, protease inhibitor cocktail tablet (Roche, Penzberg, Germany) for each 10 ml of RIPA. For protein quantification, DC™ Protein Assay kit (Bio-Rad Laboratories, CA, USA) was used, having bovine serum albumin (BSA) as standard. Absorbance was read at 750 nm (Infinite M200 multimode microplate reader, Tecan). Subsequently, 6x sample buffer (36% glycerol, 12% SDS, 0.015% bromophenol blue, 720mM dithiothreitol, 420mM Tris, pH 6.8) was added and samples were denatured (10 min, 95ºC).

Proteins were separated by SDS-polyacrylamide gel electrophoresis (SDS-PAGE), in running buffer (0.1% SDS, 192mM glycine, 25mM Tris pH 8.3), at constant voltage (80-120 V, 1h30min), using 12% acrylamide/bis-acrylamide resolving gels (0.1% SDS, 0.1% ammonium persulfate (APS), 0.04% N,N,N',N'-tetramethylethane-1,2-diamine (TEMED), 375mM Tris pH 8.8), and 5% acrylamide/bis-acrylamide stacking gels (0.1% SDS, 0.1% APS, 0.1% TEMED, 125mM Tris pH 6.8), with 1.5 mm thickness and 15 wells. The protein molecular weight marker NZYColour Protein Marker II (NZYTech, Lisbon, Portugal) was used. After, proteins were transferred to polyvinylidene difluoride (PVDF) membranes, previously activated in methanol, in transfer buffer (10% methanol, 192mM glycine, 25mM Tris pH 8.3), at constant amperage (350 mA, 1h20min). Membranes were blocked with 3% BSA in Tris buffered saline with Tween® 20 (TBS-T) (200nM Tris, 1.5M NaCl, 0.1% Tween® 20, pH 7.6) (1h, RT). Then membranes were incubated with primary antibodies (overnight, 4ºC) (Table 2). Mouse anti-vinculin antibody was used as loading control. After, membranes were washed (3 x 5 min) and incubated with secondary antibodies conjugated with horseradish peroxidase (HRP) IgG anti-rabbit (1:10 000) and IgG anti-mouse (1:10 000) (BioRad Laboratories, Hercules, CA, USA) (1h, RT) (Table 2).

Table 2. Primary antibodies used in Western Blot assays.

Antibody	Host	Company	Catalogue number	Dilution	Expected molecular weight (kDa)
Anti- tNF-κB	Rabbit	Santa Cruz	sc-372	1:1000	65
Anti- pNF-κB	Rabbit	Abcam	ab131109	1:500	65
Anti- tiκBα	Mouse	Abcam	ab12135	1:200	35.6-40
Anti- piκBα	Mouse	Cell Signalling	#9246	1:500	40
Anti- p44/42 MAPK (Erk1/2)	Rabbit	Cell Signalling	#9102	1:1000	42-44
Anti- phospho p44/42 MAPK (Erk1/2)	Rabbit	Cell Signalling	#9101	1:500	42-44
Anti- MBP	Rabbit	Cell Signalling	78896S	1:1000	12-14
Anti- PLP	Rabbit	Abcam	ab105784	1:1000	30-34
Anti- Vinculin	Mouse	Sigma	V9131	1:1000	116

Finally, after washing, proteins were revealed with Clarity™ Western ECL Substrate (Bio-Rad Laboratories), using ChemiDoc™ XRS+ imaging system with Image Lab™ software (Bio-Rad Laboratories). Membranes were stripped between incubations, in which membranes were washed in TBS-T (2×15min) and then submersed in a stripping solution (200 mM glycine, 0.1% SDS, 1% Tween® 20, 50% acetic acid glacial, pH 2.2) for 30 min (RT). Then, membranes were washed in distilled water to increase membrane pH and then washed again in TBS-T (2×15min). Resulting images were processed and analysed using ImageJ software (NIH, Bethesda, MD, USA). Results are expressed as protein levels, normalized to the percentage of control (100%).

2.10.2. Free-floating immunohistochemistry (IHC)

To assess brain demyelination, particularly in the CC, an immunohistochemistry against MBP was performed on 4 left hemisphere slices from one animal of each experimental condition.

Initially, slices were degelatinized in PBS (3×10 min, 37ºC). Afterwards, a blocking solution (6% bovine serum albumin (BSA) and 0.2% Triton™ X-100 in PBS) was applied (1h, RT). Then, slices were incubated with anti-MBP rabbit (1:200) primary antibody (Merck, Darmstadt, Germany) in 3% blocking solution (20-24h, 4ºC). On the following day, slices were washed in PBS (3 x 10 min) and incubated with

secondary antibodies anti-rabbit Alexa Fluor 568 (1:500) and DAPI (4',6'-diamidino-2-phenylindole) (1:1000) (2h, RT). After washing in PBS (3×10 min), slices were mounted on microscope slides (Superfrost™ Plus, ThermoFisher Scientific) with Mowiol, and covered with glass coverslips.

Representative images of the CC were acquired using the Zeiss Axiovert 200 Inverted Microscope (Carl Zeiss, Corp., Oberkochen, Germany), with a 5× resolution. For MBP staining, CC portions were manually delimited, using ZEN 2.5 lite software (Carl Zeiss, Corp., Oberkochen, Germany), and the area of the delimited region was determined. Results are presented normalized to the percentage of control (100%).

2.10.3. Histology: Luxol fast blue assay

To evaluate demyelinated areas in the white matter throughout EAE development, Luxol fast blue (LFB) protocol was performed on left hemisphere slices. LFB is a classical histological method that allows a distinction between myelinated and demyelinating regions, by assigning a strong blue colour to myelin[9]. Luxol staining is usually counterstained with eosin staining to distinguish myelinated from demyelinated regions.

Firstly, slices were degelatinized in PBS (15min, 37ºC), followed by an incubation with LFB Solution in water bath (overnight, 56ºC). Afterwards, excess was removed with 96% ethyl alcohol. Slices were then differentiated with a solution of lithium carbonate (20sec) and then rinsed with destilled water (1min). Subsequently, slices were washed with 70% ethyl alcohol (30sec) and counterstained with eosin (6sec) to be then washed with 70% ethyl alcohol (30sec), 96% ethyl alcohol (30sec) and 100% ethyl alcohol (30sec). Finally, slices were cleaned in xylene and mounted on microscope slides with entellan and covered with glass coverslips. Representative images were obtained using NanoZoomer-SQ Digital slide scanner C13140-01 (Hamamatsu, Japan) with a 20× resolution.

2.11. Statistical Analysis

Statistical analysis was performed using the software Graphpad Prism 6 (Graphpad, La Jolla, CA, USA). Collected data is presented as the mean ± standard error of the mean (SEM) for each experimental animal group. Ordinary one-way analyses of variance (ANOVA) followed by Bonferroni's multiple comparisons test were used to evaluate the significance of differences between means of two or more conditions, considering $p<0.05$ to represent statistically significant differences.

3. Results

3.1. EAE Clinical Scores

EAE-induction was analysed by examining daily the physical condition of the animals since the beginning of the in vivo protocol. Regarding the weight of the animals there were no differences between EAE VEH and EAE CGS until the end of the protocol (fig. 14-A).

Regarding CS analysis, it is possible to observe that EAE incidence was low (40% in EAE VEH). In fact, on average the CS per group does not overpass a CS of 1 (fig. 14-B). In comparison, the EAE onset was similar between EAE VEH and EAE CGS (fig. 14-B). In the EAE VEH group, only 2 individuals presented a CS peak of 2-3 on 20-21 days p.i, following which both animals showed partial recovery (fig. 14-C). Concerning the EAE CGS group, also only two animals developed clinical signs, starting both on day 19 p.i. (fig. 14-D). However, progression was different between animals. Animal 4 reached the peak of disease on day 20 p.i. with a maximum CS of 1-2 which was maintained until sacrificing the animal. In turn, animal 5 reached a CS peak of 2-3 on day 22 p.i. However, EAE VEH on day 22 p.i. showed a partial recovery while EAE CGS did not recover, in particular animal 5. Since we aimed at evaluating EAE at its peak on a molecular and cellular level, animals were sacrificed while at a higher CS, on day 23 p.i., to avoid a decline of CS. Animals that did not present a CS of above 1 were maintained until the end of the in vivo experimental days, to address whether they would develop the disease at a later time-point, which did not occur.

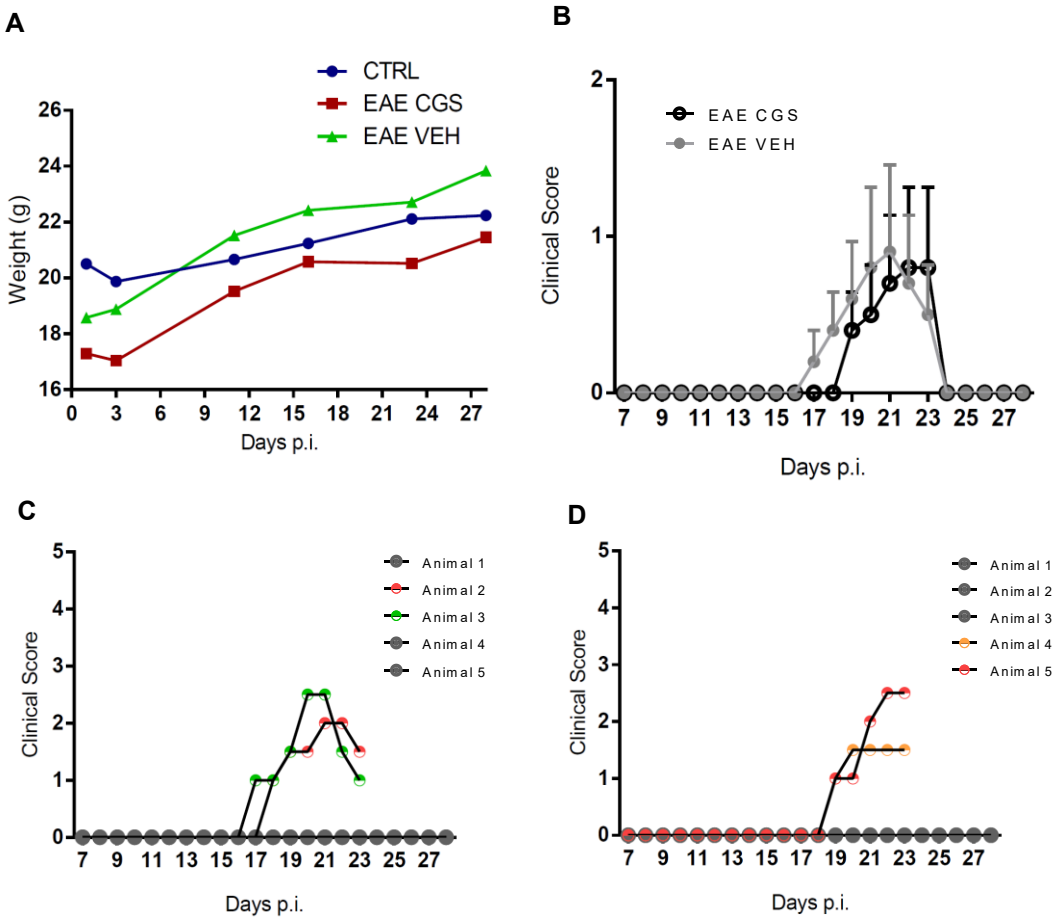

Figure 14. Clinical scores (CS) of the animals treated with vehicle solution (EAE VEH) and animals treated with CGS21680 (EAE CGS). **A –** Average weight (g) of CTRL, EAE VEH and EAE CGS groups. **B –** Average clinical scores of EAE VEH and EAE CGS groups. **C –** Individual CS of EAE VEH mice. EAE onset occurs at day 17 p.i. and maximum CS achieved was 2-3 on 20-21 days p.i.. **D –** Individual CS of EAE CGS mice. EAE onset occured on day 19 p.i. and maximum CS achieved was 2-3 on day 22 p.i..

3.2. Locomotor and exploratory activity analysis

Behavioural tests were performed to assess the model phenotype progression through alterations on locomotor and exploratory activity of the animals. A first analysis compared performances of EAE animals from both EAE VEH and EAE CGS groups and the control naïve group (CTRL). In a second analysis, EAE VEH and EAE CGS animals with CS=0 score were excluded from the group's mean calculation to better assess the effect of the phenotype on performance parameters. It is worth saying that, although a tendency is visible, these results are not significant due to low experimental *n* (EAE VEH CS>1, EAE CGS CS>1, n=2). Since EAE VEH and EAE CGS animals with CS>1 were sacrificed at day 23 p.i., the behavioural analysis comparison between groups was performed until day 22 p.i..

3.2.1. EAE VEH and EAE CGS animals showed impaired PT performance on day 21 p.i.

PT allowed the assessment of locomotor activity by placing animals head-upwards on a pole to evaluate their ability to descend it. Time to descend ($t_{descend}$), time to orient (t_{orient}) and total time of the task (t_{total}) were registerd.

When analyzing all animals (n=5), most of the results did not differ between groups. However, EAE VEH group showed an increase in t_{orient} in comparison with the CTRL group on day 21 p.i. (CTRL: 1.75 ± 0.27 s; day 21 p.i. – EAE VEH: 5.97 ± 1.83 s; *p<0.05, n=5, fig. 15-A). Moreover, EAE CGS group exhibited the lowest value of $t_{descend}$ on day 14 p.i. (CTRL: 10.1 ± 1.03 s; EAE VEH: 7.35 ± 1.11; EAE CGS: 5.35 ± 0.232 s; #p<0.05, n=5, fig. 15-B) and of t_{total} (CTRL: 15.9 ± 1.81 s; EAE VEH: 11.3 ± 1.43; EAE CGS: 10.4 ± 0.34 s; #p<0.05, n=5, fig. 15-C). In addition, a noteworthy decrease of t_{total} in the CTRL group was seen along the experimental protocol (CTRL: day 14 p.i. – 15.90 ± 1.814 s; day 17 p.i. – 10.70 ± 0.7961 s; day 21 p.i. – 9.375 ± 1.073 s, *p<0.05, **p<0.01, n=5, fig. 15-C). Overall, these results were not very conclusive since a general decrease in PT behavioural parameters was observed in all groups until day 17 p.i., which can be due to animals learning the task. On day 21 p.i., a minor increase is seen in EAE VEH t_{orient}, while on $t_{descend}$ variations are not elucidative.

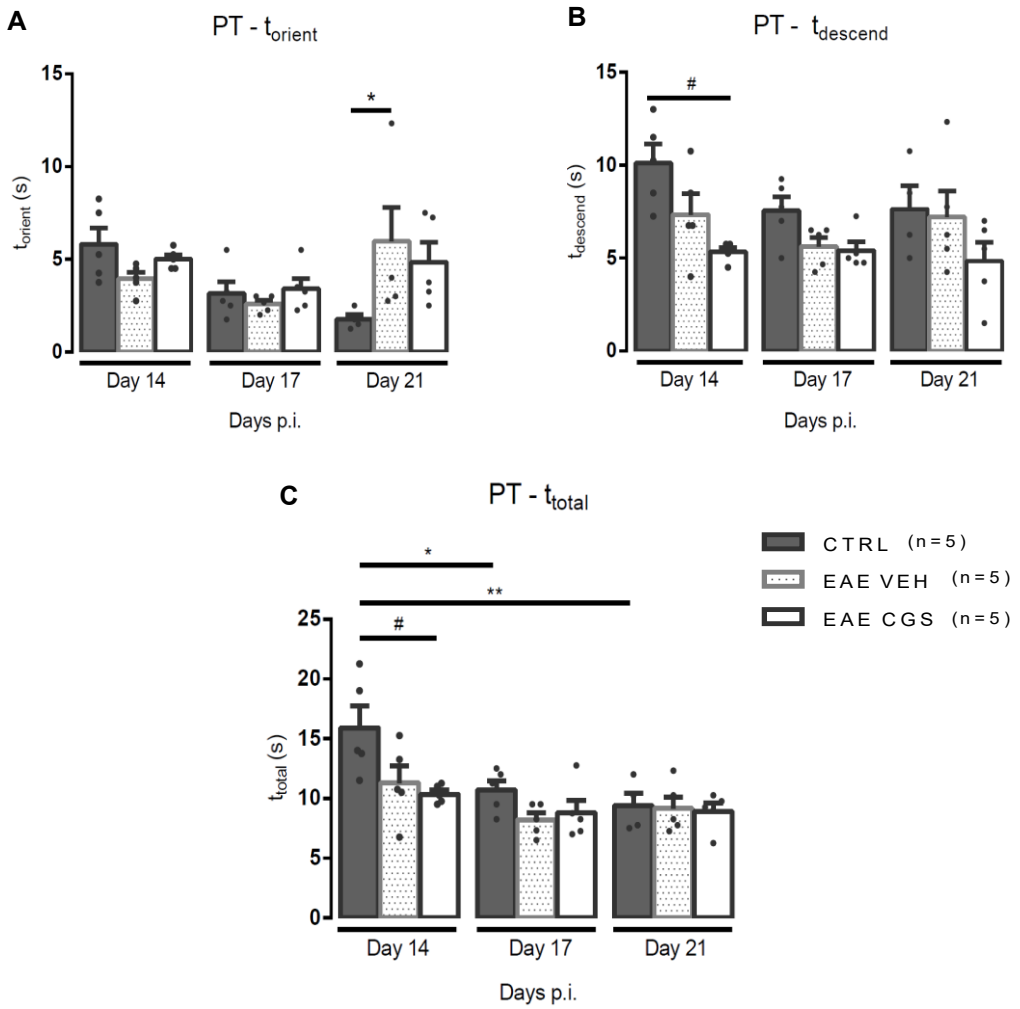

Figure 15. Pole test performance analysis. t_{orient} **(A)**, $t_{descend}$ **(B)** and t_{total} **(C)** parameters were quantified. **A –** EAE VEH group showed an increase in comparison with the CTRL group on day 21 p.i. (*p<0.05, ordinary one-way ANOVA followed by Bonferroni's multiple comparison test). **B –** EAE CGS group exhibited the lowest value of $t_{descend}$ on day 14 p.i. ($^{\#}$p<0.05, n=5, ordinary one-way ANOVA followed by Bonferroni's multiple comparison test). **C -** CTRL group t_{total} decreased along the experimental protocol (*p<0.05, **p<0.01, ordinary one-way ANOVA followed by Bonferroni's multiple comparison test). EAE CGS group showed the lowest t_{total} value on day 14 p.i. (**$^{\#}$**p<0.05, ordinary one-way ANOVA followed by Bonferroni's multiple comparison test). Data is presented as mean ± SEM (n=5).

Since the behavioural analysis with all animals was inconclusive only individuals with CS>1 from EAE CGS and EAE VEH groups were analysed (n=2). The most relevant result concerns a tendency of t_{orient} to increase from day 17 to day 21 p.i. in both EAE CGS and EAE VEH groups (EAE VEH: day 17 p.i. – 2.12 s; day 21 p.i. – 10.04 s; EAE CGS: day 17 p.i. – 4.50 s; day 21 p.i. – 7.38 s, n=2, fig.16-A), as well as an increase in $t_{descend}$ in EAE VEH group (day 17 p.i. – 5.25 s; day 21 p.i. – 10.0 s; n=2, fig.16-B). These changes are in accordance with the CS development observed in both groups. In fact, motor impairment worsened with EAE progression, while the locomotor capacity of the animals to efficiently complete the task was disturbed. EAE VEH group had a peak of disease at day 21 p.i., which correlates with the significant impairment in performing the task, with an increase in both t_{orient} and $t_{descend}$. Regarding the EAE CGS group, this impairment is not as visible, particularly in the $t_{descend}$ parameter, as

animals did not present as high CS as the EAE VEH group. Moreover, on day 21 p.i., both EAE VEH and EAE CGS groups show a higher t_{orient} than the CTRL group (CTRL: 1.75 ± 0.27 s; EAE VEH: 10.04 s; EAE CGS: 7.38 s; n=5, n=2, fig.16-A).

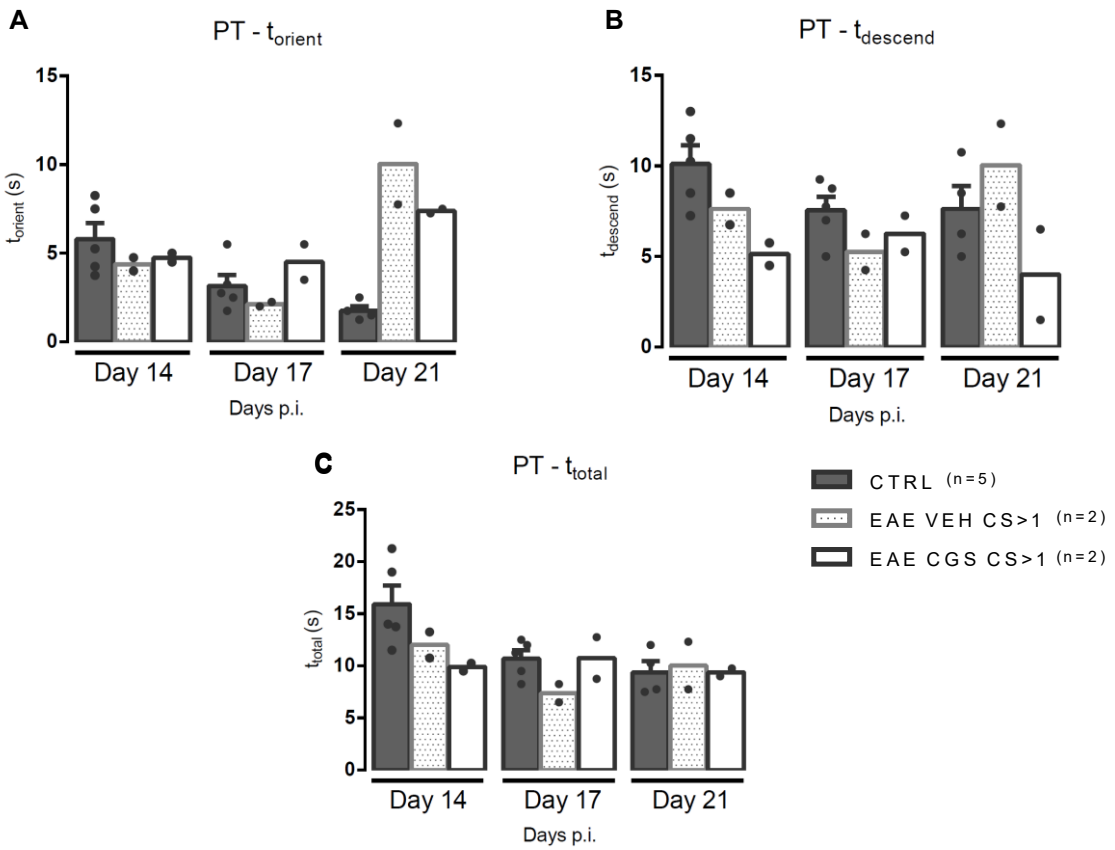

Figure 16. EAE CGS and VEH animals with CS>1 showed impaired performance in the PT on day 21 p.i., coinciding with EAE phenotype worsening. t_{orient} **(A)**, $t_{descend}$ **(B)** and t_{total} **(C)** parameters were quantified. **A –** EAE VEH and EAE CGS groups showed an increase in t_{orient} from day 17 p.i. to day 21 p.i.. **B –** EAE VEH group showed an increase in $t_{descend}$ from day 17 p.i. to day 21 p.i.. **C –** No variations were observed in t_{total} between EAE VEH and EAE CGS groups. Data is presented as mean (n=2) or as mean ± SEM (n=5).

3.2.2. EAE VEH and EAE CGS animals showed impaired RR performance on day 21 p.i.

While analyzing the performance of all animals on the rotarod (n=5) on day 17 and 21 p.i., a small tendency of decrease in EAE VEH group t_{fall} was observed (EAE VEH: day 17 p.i. – 85.4 ± 12.8 s; day 21 p.i. – 52.6 ± 4.68 s, n=5, fig.17-A) as well as in maximum rotation (EAE VEH: day 17 p.i. – 14.0 ± 1.53 rpm; day 21 p.i. – 10.2 ± 0.58 rpm, n=5, fig.17-B). Contrarily, an overall increase was observed in the CTRL group performance parameters. No major variations were observed in the CGS group results. Moreover, on day 21 p.i. the CTRL showed higher t_{fall} (CTRL: 93.9 ± 16.3 s; EAE VEH: 52.6 ± 4.68 s; EAE CGS: 70.1 ± 15.8 s; n=5, fig.17-A) and maximum rotation values (CTRL: 15.3 ± 1.98 s; EAE VEH: 10.2 ± 0.58 rpm; EAE CGS: 12.3 ± 1.96; n=5, fig.17-B).

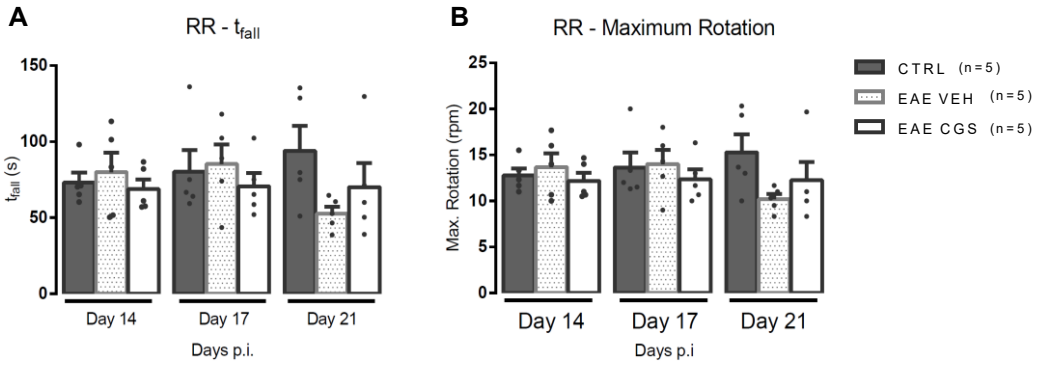

Figure 17. Rotarod performance analysis. t_{fall} **(A)** and maximum rotation **(B)** were quantified **A –** From day 17 p.i. to day 21 p.i. EAE VEH group showed a tendency to decrease in t_{fall} from day 17 p.i. to day 21 p.i.. The CTRL group showed a higher t_{fall} at day 21 p.i.. **B –** A decrease was observed in maximum rotation value for the EAE VEH group from day 17 p.i. to day 21 p.i.. CTRL group showed maximum rotation values at day 21 p.i.. Data is presented as mean ± SEM (n=5).

As the analysis for the PT, the EAE VEH and EAE CGS groups with CS>1 (n=2), were analysed. Results show a tendency in both EAE VEH and EAE CGS groups for a decrease in t_{fall} (EAE VEH: day 17 p.i. –110.2 s; day 21 p.i. – 53.5 s; EAE CGS: day 17 p.i. – 77.2 s; day 21 p.i. – 44.7 s; n=2, fig.18-A) and maximum rotation (EAE VEH: day 17 p.i. – 17.0 rpm; day 21 p.i. –10.3 rpm; EAE CGS: day 17 p.i. –13.2 rpm; day 21 p.i. – 9.2 rpm; n=2, fig.18-B). This time point coincides with the peak of CS in the EAE VEH group and progression of CS in the EAE CGS group. In fact, the capacity of the animals to stand longer on the RR declined, as t_{fall} and max. rotation mean values decreased. Nonetheless, when comparing EAE VEH with EAE CGS no significant differences were observed. Again, regarding the CTRL group, an improvement in performance was observed along the experimental protocol, as animals lasted longer on the RR, meaning an adaptation to the task.

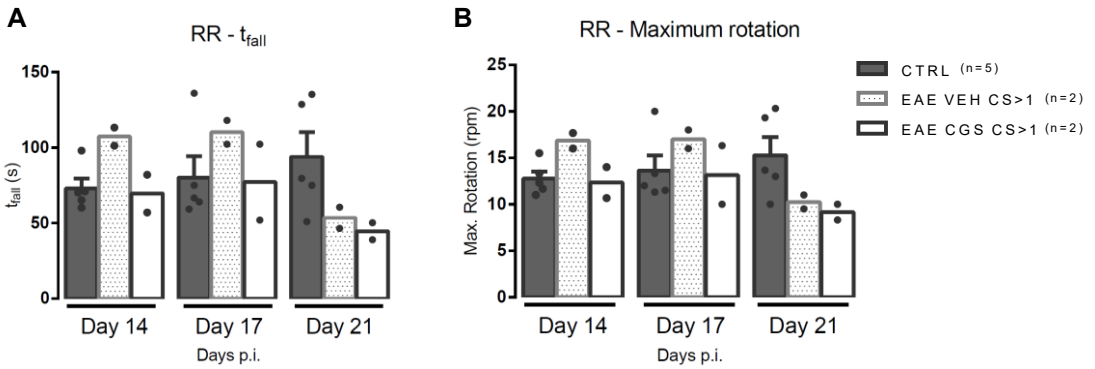

Figure 18. EAE CGS and VEH animals with CS>1 showed impaired performance in the RR on day 21 p.i., coinciding with EAE phenotype worsening. A – A decrease of t_{fall} was observed in both EAE VEH and EAE CGS groups from day 17 p.i. to day 21 p.i.. **B –** Maximum rotation value was decreased from day 17 p.i. to day 21 p.i. in both EAE VEH and EAE CGS groups. Data is presented as mean (n=2) or as mean ± SEM (n=5).

3.2.3. EAE CGS and EAE VEH animals showed impaired locomotor and exploratory activity on day 18 and 22 p.i.

Regarding travelled distance, a minor tendency of decrease was seen in all experimental groups on day 18 p.i., with EAE CGS group presenting the lowest mean values. Moreover, these values were maintained from day 18 to day 22 p.i. (day 15 p.i. – CTRL: 34.02 ± 1.78 m; EAE VEH: 41.76 ± 6.63 m; EAE CGS: 23.1 ± 2.6 m; day 18 p.i. – CTRL: 27.7 ± 3.36 m; EAE VEH: 31.9 ± 11.3 m; EAE CGS: 15.42 ± 1.40 m; day 22 p.i. – CTRL: 28.12 ± 2.23; EAE VEH: 28.0 ± 10.1; EAE CGS: 16.02 ± 1.83; n=5, fig.19-A). Variations of the number (nr.) of crossings were almost negligible, with EAE CGS group presenting the lowest values of the three experimental groups.

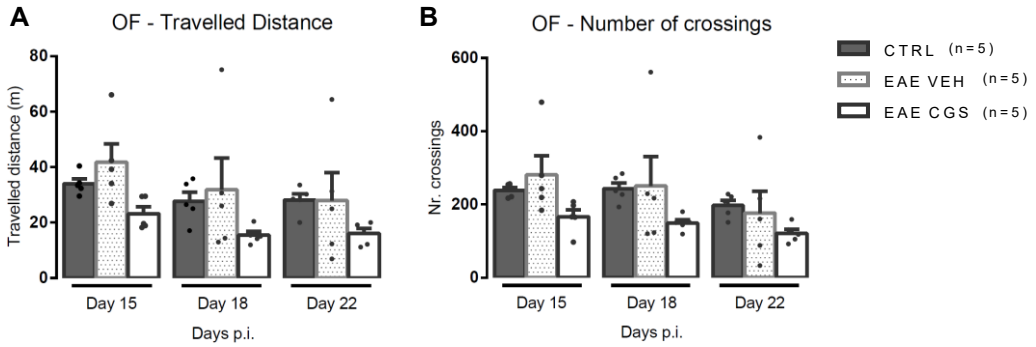

Figure 19. Open field performance analysis. Travelled distance **(A)** and nr. of crossings **(B)** were quantified. **A –** Travelled distance showed a minor decrease in all experimental groups on day 18 p.i., which was maintained from day 18 to 22 p.i.. **B –** Variations in the nr. of crossings were not noteworthy. Data is presented as mean ± SEM (n=5).

When considering only EAE VEH and EAE CGS animals with CS>1 (n=2), from day 15 to day 22 p.i., a considerable tendency of decrease in the travelled distance in both EAE VEH and EAE CGS groups was seen (EAE VEH: day 15 p.i. – 30.51 m; day 18 p.i. – 13.67 m; day 22 p.i. – 9.620 m; EAE CGS: day 15 p.i. – 29.47 m; day 18 p.i. – 17.96 m; day 22 p.i. – 11.65 m; n=2, fig.20-A). This decrease, although less striking, is also seen in the nr. of crossings (EAE VEH: day 15 p.i. – 201.5; day 18 p.i. – 121.5; day 22 p.i. – 60.5; EAE CGS: day 15 p.i. – 202.0; day 18 p.i. – 165; day 22 p.i. – 105.0; n=2, fig.20-B). Altogether, these data suggest that a higher CS has influence in the exploratory and motor activity of the animals, being particularly relevant that day 18 p.i. coincides with the appearance of EAE phenotype on EAE VEH group, which corresponds to a decrease in travelled distance and nr. of crossings. Nonetheless, this decrease was also observed in EAE CGS animals, that at this time point still did not display EAE phenotype.

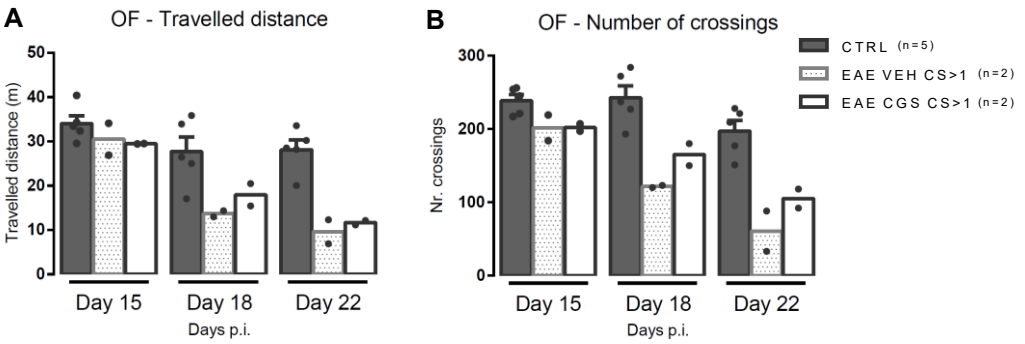

Figure 20. EAE VEH and EAE CGS animals with CS>1 showed impaired locomotor and exploratory activity as EAE phenotype aggravates, from day 18 to day 22 pi.. Travelled distance **(A)** and nr. of crossings **(B)** were quantified. **A –** EAE VEH and EAE CGS groups showed a tendency of decrease in travelled distance from day 15 to day 22 p.i.. **B –** A decrease was also in the nr. of crossings in EAE VEH and EAE CGS groups from day 15 to day 22 p.i.. Data is presented as mean (n=2) or as mean ± SEM (n=5).

3.3. Cellular and molecular analysis

It was essential to assess the role of the $A_{2A}R$ agonist action under EAE pathogenesis. Hence, further molecular and cellular analysis were performed in order to better assess differences in EAE CGS versus EAE VEH mice.

Myelin levels were analysed through immunohistochemistry for MBP staining, LFB histological assay and western blotting for myelin proteins quantification, as MBP and PLP. $A_{2A}R$ agonist activation effect on oligodendrocytes remyelinating action and inflammation was assessed by western blot techniques to quantify Nf-κB and MAPK/ERK1/2 proteins, to evaluate these signaling pathways.

3.3.1. WB analysis

Western blot assays were performed using tissue lysates from four brain areas: cortex, striatum, CC and SVZ. These particular areas were selected for covering, not only the neurogenic niche of interest of our study, SVZ, but for being the most demyelinated areas under EAE pathogenesis[60,107]

3.3.1.1. MBP and PLP levels were not changed in EAE VEH and EAE CGS animals

As aforementioned, EAE pathogenesis exacerbates inflammatory response inducing the deterioration of the myelin sheath. Therefore, to assess de- and remyelination processes under EAE pathophysiological conditions with and without $A_{2A}R$ agonist treatment, MBP and PLP protein levels, the most abundant proteins of the myelin sheath and highly responsible for its compactness[108,109], were assessed by western blot techniques.

Regarding PLP levels in all tested conditions and in different brain areas, no major changes were found. Cortical samples from EAE CGS animals with CS=0 presented a tendency for a higher PLP protein value comparatively to EAE CGS animals with CS>1 (EAE CGS: CS=0: 145.4 %; CS>1: 43.9 %; n=1; n=2, respectively, fig.21-A). However, the opposite was seen in samples from EAE VEH animals, with samples from animals with CS>1 presenting higher PLP protein levels (EAE VEH: CS=0: 46.10 %; CS>1: 126.0 %; n=2, fig.21-A). Moreover, cortex from CTRL animals had a tendency for lower PLP protein levels than these 2 groups (CTRL: 100.0 ± 4.743 %; EAE CGS CS=0: 145.4 %; EAE VEH CS>1: 126.0 %; n=3; n=2, respectively, fig. 21-A). Considering striatal samples, EAE VEH and EAE CGS animals with CS=0 presented higher PLP values than EAE VEH and EAE CGS animals with CS>1, respectively (EAE VEH: CS=0: 131.0 %, n=3; CS>1: 98.25 %, n=2; EAE CGS: CS=0: 112.0 %; CS>1: 61.20 %; n=2, fig. 21-B). Regarding CC samples, a similar tendency is observed comparing with cortical samples, although differences being much less prominent and protein levels being considerably lower than in cortical or in striatal samples.

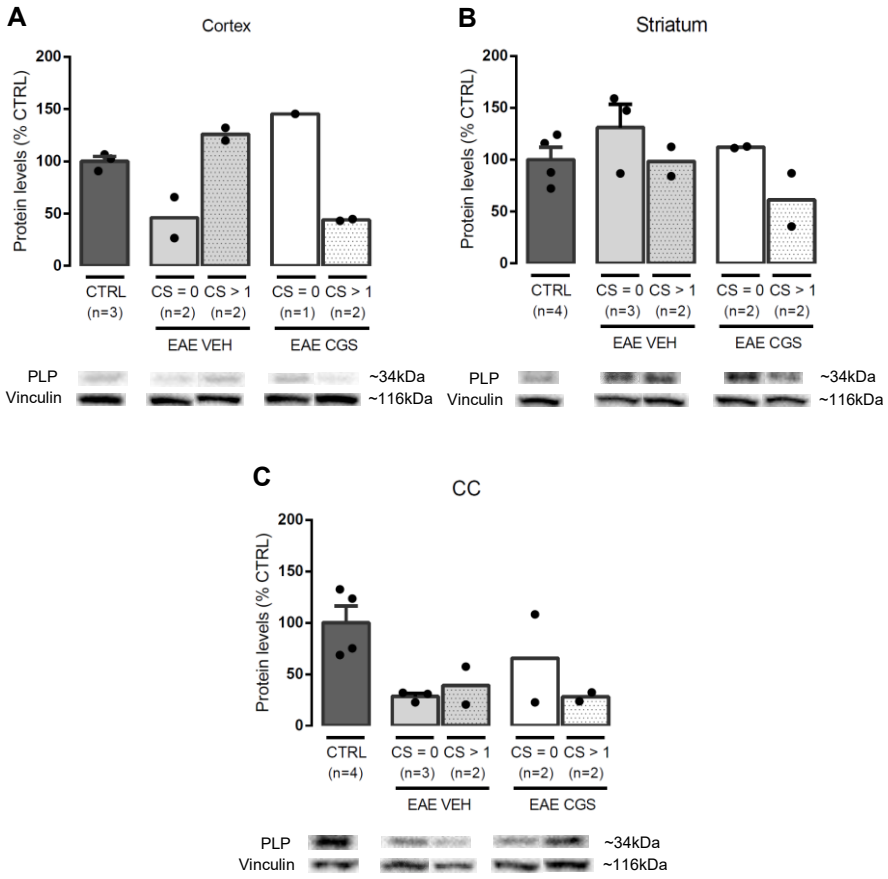

Figure 21. Myelin protein PLP levels were not altered in EAE VEH and EAE CGS animals with CS>1. Cortical **(A)**, striatal **(B)** and CC **(C)** lysate samples were analysed. **A –** In cortical samples, EAE CGS animals with CS=0 presented higher PLP protein levels than EAE CGS animals with CS>1. EAE VEH animals with CS>1 showed higher PLP values than EAE VEH animals with CS=0. **B –** In striatal samples, EAE VEH and EAE CGS animals with CS=0 showed higher PLP protein levels than EAE VEH and EAE CGS animals with CS>1, respectively. **C –** In CC samples, PLP protein levels did not change between EAE VEH or EAE CGS with CS=0 or CS>1. Data is presented as mean (n=1-2) or as mean ± SEM (n=3-5).

Concerning MBP cortical samples, these have a similar protein level in all experimental conditions, with no noteworthy differences. Striatal samples presented a similar tendency of decline of MBP levels in both EAE VEH and EAE CGS animals with CS>1 in comparison with the respective EAE VEH and EAE CGS animals with CS=0 (EAE VEH: CS=0: 87.90 %; CS>1: 68.65 %; n=2-3; EAE CGS: CS=0: 68.30 %; CS>1: 58.20 %; n=2, fig.22-B). The same tendency is seen in SVZ samples (EAE VEH: CS=0: 108.1 %; CS>1: 51.45 %; n=2-3; EAE CGS: CS=0: 67.55 %; CS>1: 39.80 %; n=2, fig.22-C).

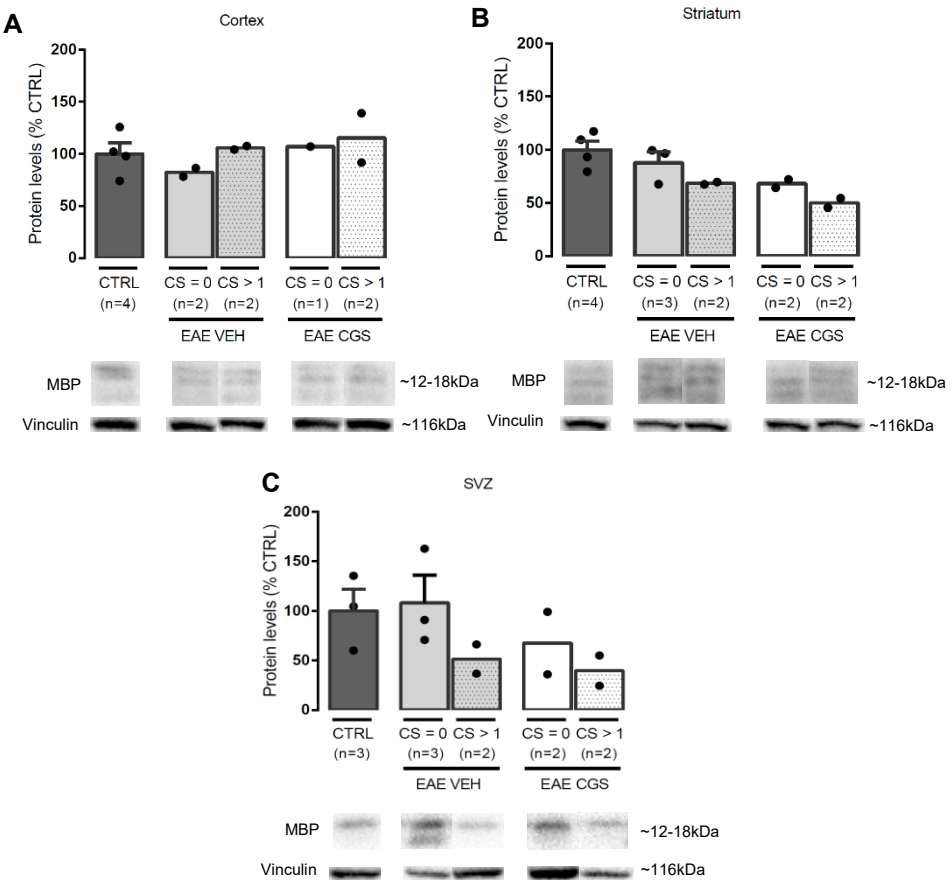

Figure 22. Myelin protein MBP levels were not altered in EAE VEH and EAE CGS animals with CS>1. Cortical **(A)**, striatal **(B)** and CC **(C)** lysate samples were analysed. **A –** In cortical samples, MBP protein levels were similar between groups. **B –** In striatum samples, both EAE VEH CS>1 and EAE CGS CS>1 groups showed lower MBP protein levels than the corresponding EAE VEH and EAE CGS groups with CS=0. **C –** In SVZ samples, the tendency was similar to striatal samples. Data is presented as mean (n=1-2) or as mean ± SEM (n=3-5).

Furthermore, when comparing MBP and PLP levels in the same brain region there is no coherence and no tendency can be inferred. In addition, no major differences are observed when comparing EAE VEH and EAE CGS groups.

3.3.1.2. EAE VEH and EAE CGS animals showed no changes in NF-κB signaling pathway

To assess the role of the $A_{2A}R$ agonist in the activation of the nuclear factor NF-κB signaling pathway, its phosphorylated and total forms, pNF-κB and tNF-κB as well as the phosphorylated and total forms of its inhibitory protein IκBα were quantified. Protein levels were quantified as a ratio between the phosphorylated and the total form.

Cortical samples presented similar protein levels of pNF-κB between conditions (fig.23-A). Observing striatal samples, no significant changes in pNF-κB protein levels were seen between groups, despite a slight increase in EAE CGS animals with CS>1 when compared with animals with CS=0 (EAE CGS: CS=0: 67.30 %; CS>1: 100.0 %; n=2, n=1, respectively, fig. 23-B). Considering CC samples, although variations are not prominent, a tendency to an increase in EAE VEH animals with CS>1 was seen when compared to EAE VEH animals with CS=0 (EAE VEH: CS=0: 68.67 %; CS>1: 129.5 %; n=3, n=2, respectively, fig. 23-C). In addition, in CC samples, EAE CGS animals with CS=0 also presented higher NF-κB protein levels when comparing with EAE CGS animals with CS>1 (EAE CGS: CS=0: 121.5 %; CS>1: 85.90 %; n=2, fig. 23-C). For SVZ samples, there were no apparent changes in all experimental conditions (fig. 23-D).

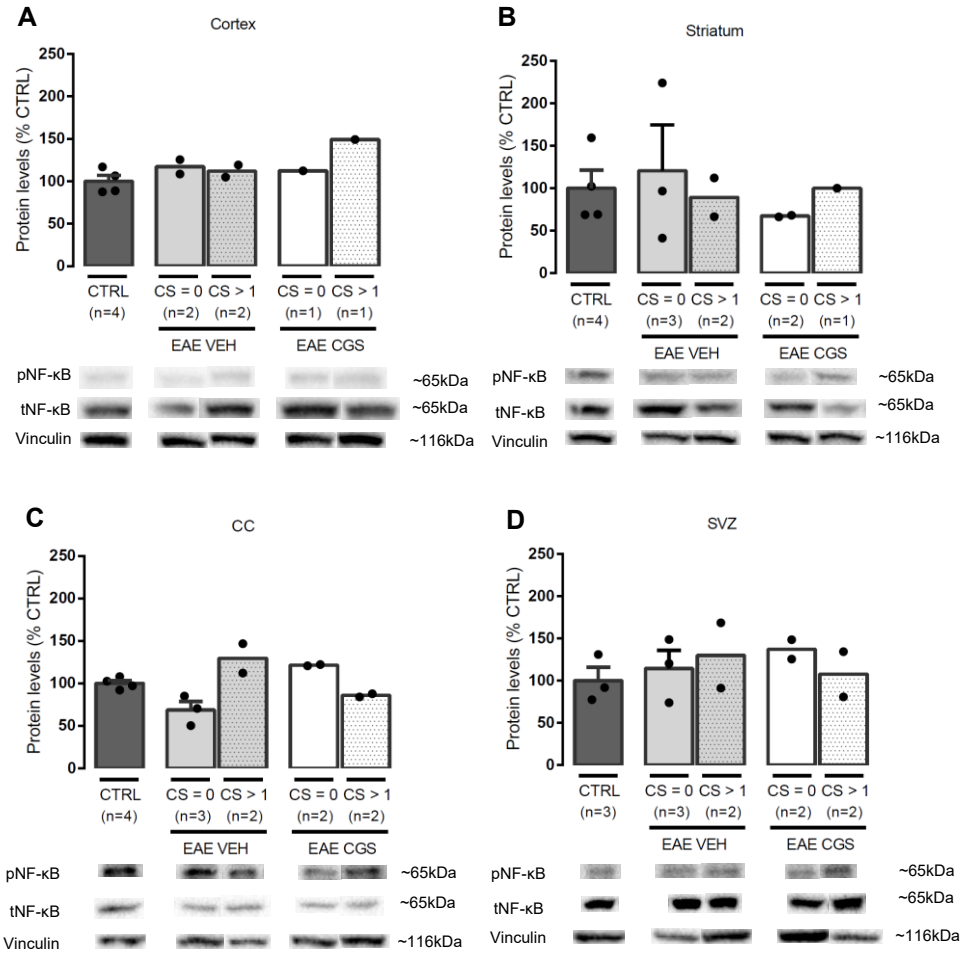

Figure 23. pNF-κB levels were not altered in EAE VEH and CGS animals. Cortex lysate samples results **(A)**, striatum lysate samples results **(B)**, CC lysate samples results **(C)** and SVZ lysate samples results **(D)**. **A –** In cortex samples, pNF-κB levels did not vary between groups. **B –** In striatal samples, EAE CGS CS>1 condition presented higher pNF-κB levels than the EAE CGS CS=0 group (EAE CGS: CS=0: 67.30 %; CS>1: 100.0 %; n=2, n=1, respectively). **C –** In CC samples, EAE VEH CS>1 showed an increase in pNF-κB value comparatively to EAE VEH CS=0 (EAE VEH: CS=0: 68.67 %; CS>1: 129.5 %; n=3, n=2, respectively)**. D –** In SVZ samples, there were no apparent changes in all experimental conditions. Data is presented as mean (n=1-2) and as mean ± SEM (n=3-5).

Regarding the pIκBα protein levels, a similar pattern of variation is observed when comparing with pNF-κB. In fact, comparing the changes of these two proteins in cortical, striatal and SVZ samples, the same tendency is observed, although with a higher amplitude of variation in pIκBα protein levels. In cortical and striatal samples, EAE VEH animals with CS=0 show higher protein levels in comparison with EAE VEH animals with CS>1 (cortex - EAE VEH: CS=0: 188.5 %; CS>1: 115.7 %; striatum - EAE VEH: CS=0: 165.2 %; CS>1: 118.7 %; n=2, fig.24-A, B). While in EAE CGS animals the opposite was observed (striatum - EAE CGS: CS=0: 95.75 %; CS>1: 143.3 %; n=2, n=1, respectively, fig.24-B). Regarding SVZ samples, the opposite tendency was observed, with EAE CGS animals with CS=0 showing higher pIκBα protein levels with EAE CGS animals with CS>1 (EAE CGS: CS=0: 130.7 %; CS>1: 53.5 %; n=2, respectively, fig.24-D). Contrarily, pIκBα protein levels in CC samples did not show any substantial variation between groups.

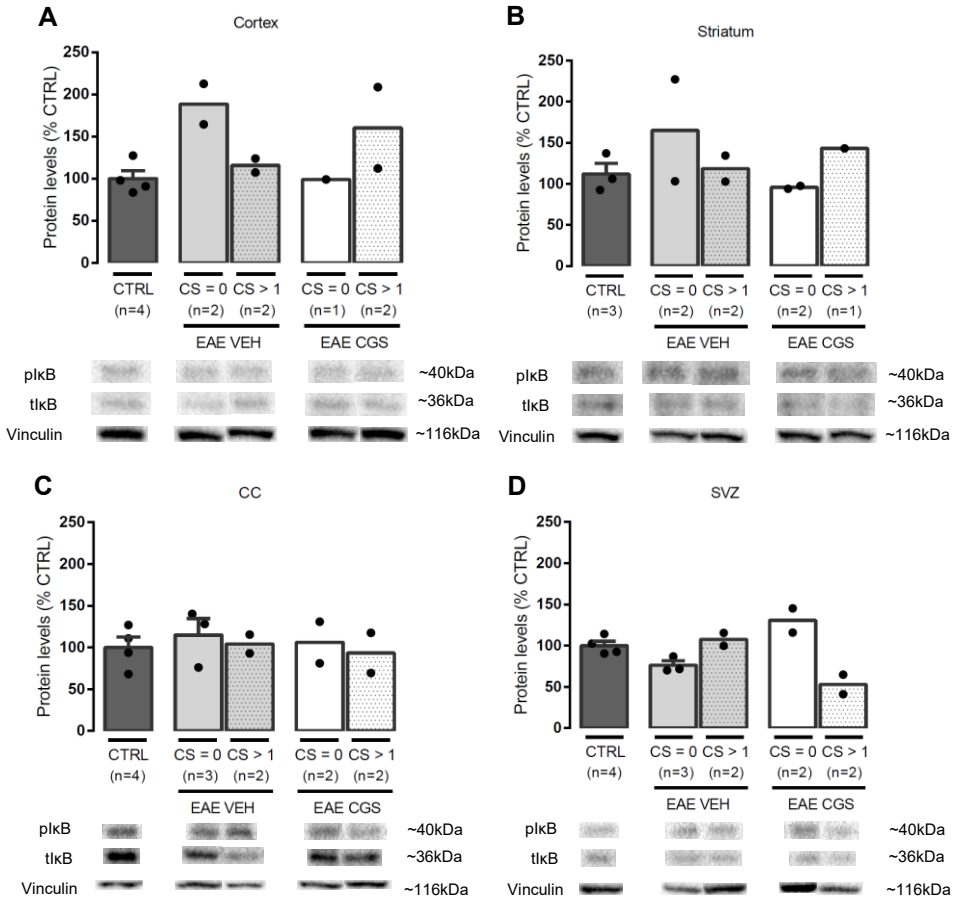

Figure 24. pIκBα levels were not altered in EAE VEH and CGS animals. Cortical lysate samples results **(A)**, striatal lysate samples results **(B)**, CC lysate samples results **(C)** and SVZ lysate samples results **(D)**. **A –** In cortical samples, EAE VEH animals with CS=0 showed increased pIκBα levels than EAE VEH animals with CS>1 (EAE VEH: CS=0: 188.5 %; CS>1: 115.7 %; n=2); **B –** Striatal samples showed a similar tendency than cortical samples (EAE VEH CS=0: 165.2 %; EAE VEH CS>1: 118.7 %; n=2), while EAE CGS CS>1 present higher values than EAE CGS CS=0 (EAE CGS CS=0: 95.75 %; EAE CGS CS>1: 143.3 %; n=2, n=1, respectively); **C –** In CC samples, different groups showed no alterations in pIκBα levels. **D –** In turn, in SVZ samples, EAE CGS CS=0 presented higher values than EAE CGS CS>1 (EAE CGS: CS=0: 130.7 %; CS>1: 53.5 %; n=2, n=1, respectively). Data is presented as mean (n=1-2) and as mean ± SEM (n=3-5).

3.3.1.3. EAE CGS animals showed no changes in the MAPK/ERK(1/2) signaling pathway

To assess whether $A_{2A}R$ agonist promotes the activation of the MAPK/ERK(1/2) signaling pathway, pERK(1/2) and tERK(1/2) were quantified. Protein levels were quantified as a ratio between the phosphorylated and the total form.

No major changes were seen in pERK protein levels. However, a tendency for an increase in EAE CGS animals with CS>1 comparatively to EAE CGS animals with CS=0 is observed in cortical (EAE CGS: CS=0: 50.70 %; CS>1: 137.9 %; n=1, n=2, respectively; fig.25-A), striatal (EAE CGS: CS=0: 50.50 %; CS>1: 73.00 %; n=2; fig.25-B) and CC samples (EAE CGS: CS=0: 58.0 %; CS>1: 113.8 %; n=2, n=1, respectively; fig.25-C). Oppositely, in SVZ samples protein levels do not show any substantial variations between groups (fig.25-D). pERK protein levels in EAE VEH groups are very similar to CTRL groups in all brain areas studied.

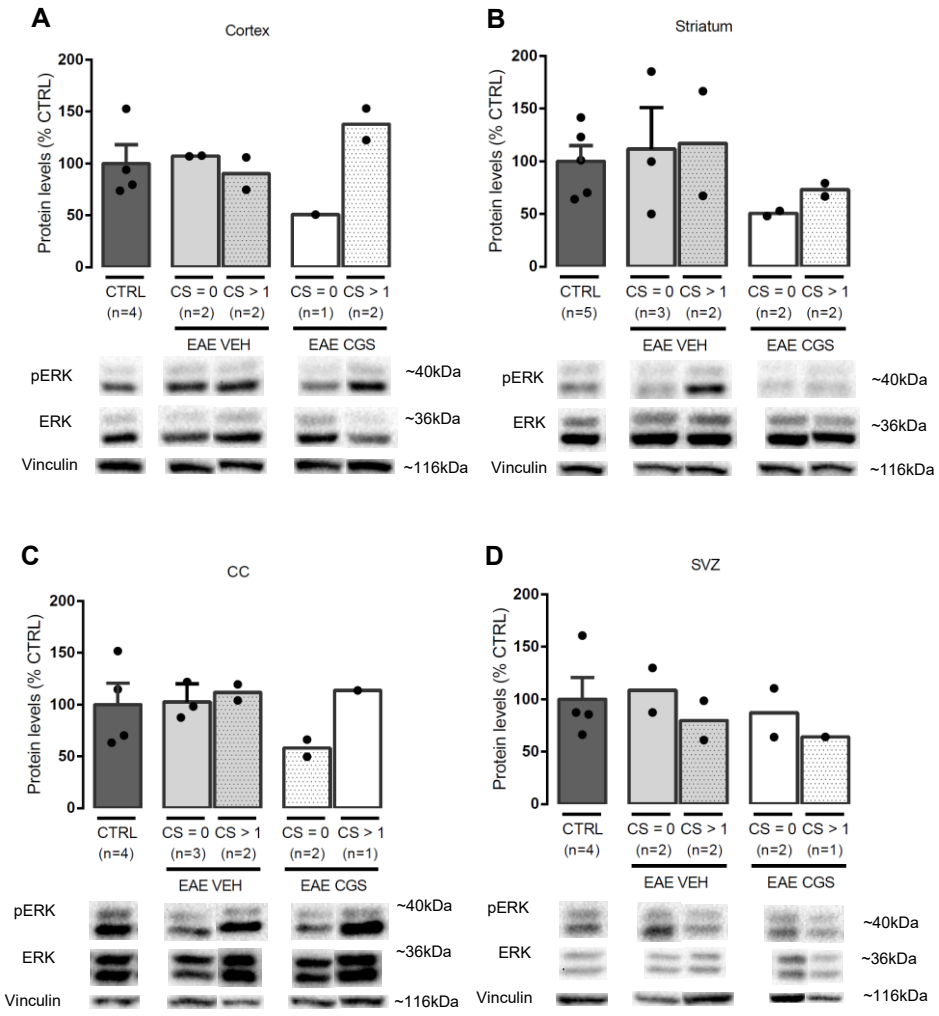

Figure 25. pERK(1/2) levels were not altered in EAE CGS animals. Cortical **(A)**, striatal **(B)**, CC **(C)** and SVZ **(D)** lysate samples were analysed. **A, C –** In cortical and CC samples EAE CGS CS>1 group showed increased pERK(1/2) protein levels than EAE CGS CS=0. **B –** In striatal samples the increase in pERK(1/2) protein levels in EAE CGS CS>1 was less evident. **D –** In SVZ samples, pERK(1/2) protein levels did not show any substantial variation between groups. Data is presented as mean (n=1-2) or as mean ± SEM (n=3-5).

3.3.2. MBP protein levels in the CC remained unaltered in EAE VEH and EAE CGS animals with CS>1

To assess demyelination in the CC, an immunohistochemistry for MBP was performed in one animal of each condition: CTRL, EAE VEH and EAE CGS with CS=0, EAE VEH and EAE CGS with CS>1. In sum, no significant differences were observed between conditions (CTRL: 100.0 ± 10.48 %; EAE VEH: CS=0: 105.9 ± 17.44 %; CS>1: 85.40 ± 12.83 %; EAE CGS: CS=0: 68.75 ± 4.784; CS>1: 91.20 ± 12.76 %; n=1; fig.26-B).

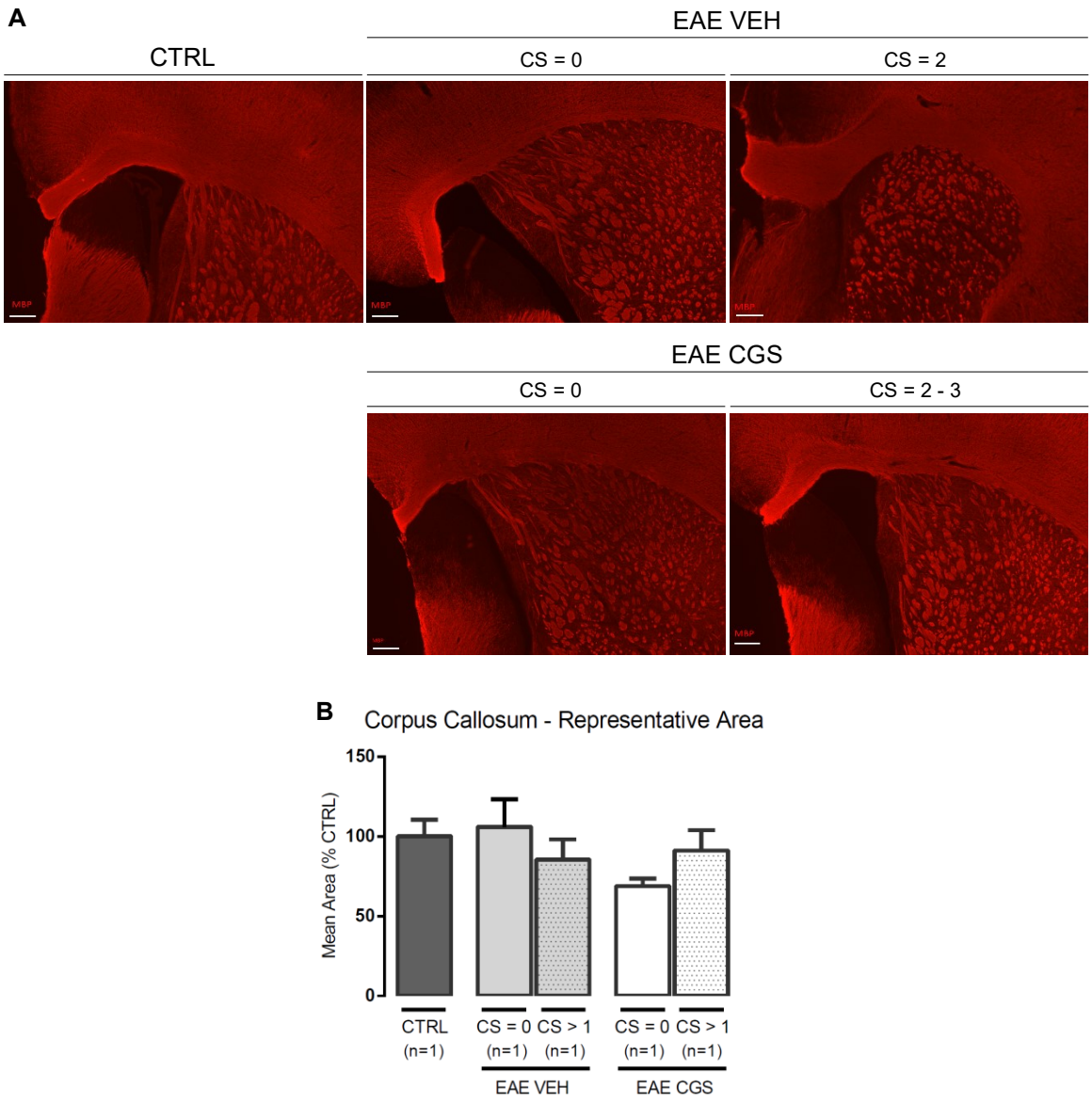

Figure 26. MBP expression in the CC remained unaltered between CTRL and EAE VEH or EAE CGS conditions. A – Representative images for MBP staining for CTRL, EAE VEH CS=0, EAE VEH CS>1, EAE CGS CS=0 and EAE CGS CS>1 mice; **B –** Mean area of MBP staining in the CC, normalized to the percentage of control (%CTRL). No differences were observed in between CTRL, EAE VEH or EAE CGS animals with CS=0 or CS>1. Data is expressed as mean. Scale bar: 200 µm.

3.3.3. Demyelination was not observed in EAE VEH and EAE CGS animals with CS>1

LFB staining was used to complement the assessment of demyelination in the CNS. This protocol is extremely effective in distinguishing demyelinated regions in the spinal cord and brain, by attributing the colour blue to myelin.

Again, to assess demyelination and remyelination, LFB staining was performed in slices from one animal of each condition: CTRL, EAE VEH and EAE CGS with CS=0, EAE VEH and EAE CS with CS=2,2-3. In general, no significant differences were observed between conditions. Peripheral cortical regions display a more rose tone, when compared with ventral regions of the cortex, and the CC maintains an intense blue colour, in all experimental conditions. Blue colour staining appears to be lighter in both EAE VEH and EAE CGS animals with CS>1 than in CTRL or EAE slices from animals with CS=0 slices, although colour distribution remains quite similar. Taken together, EAE model pathophysiology did not seem to cause any apparent effects on myelin levels in the brain.

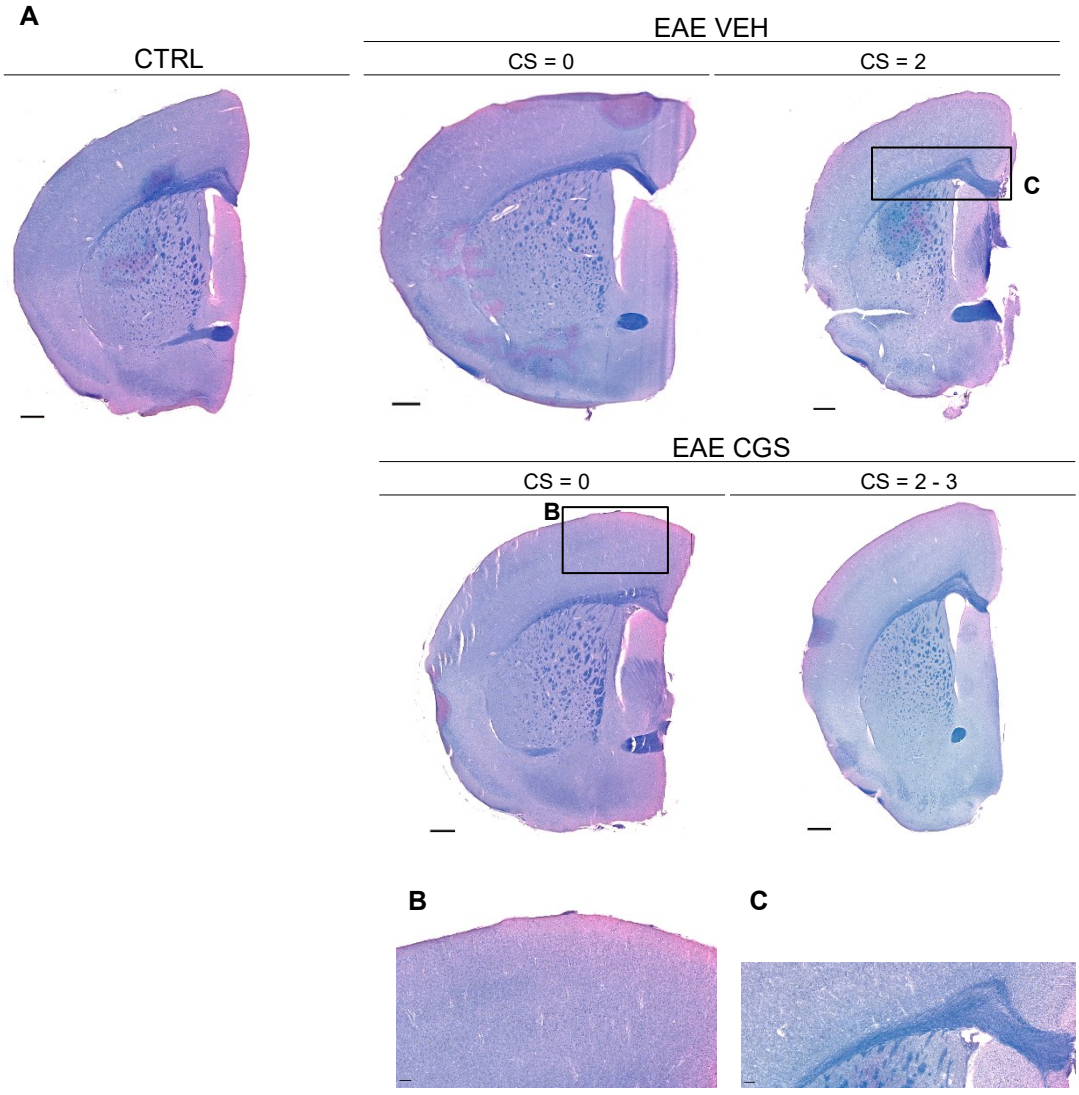

Figure 27. Myelin levels in EAE VEH and EAE CGS animals remained unaltered in comparison to CTRL animals. A – Representative images for LFB staining. Scale bar: 500 µm. **B, C** – are magnifications of squares B (cortex of EAE CGS CS=0) and C (CC of EAE VEH CS=2). Scale bar: 100 µm.

4. Discussion

In this experimental work, I aimed at understanding the role of adenosine A_{2A} Receptors in enhancing maturation and differentiation of OPCs into OLGs, under EAE model pathogenic conditions. Myelin levels were evaluated to assess the putative remyelination response, while behavioural tests were performed to analyse whether $A_{2A}R$ have an effect on oligodendrocyte activity and on the regulation of the neuroinflammatory response that could improve EAE phenotype, leading to an improvement of locomotor and exploratory activity in EAE animals.

The first step of our work intended to efficiently induce the EAE model on female C57BL/6 mice ten-weeks-old, using a commercialized induction kit by Hooke Laboratories, composed of a MOG_{35-55} rat emulsion in CFA with *M. tuberculosis* and PTX. However, incidence was only of 40% in EAE VEH, which, reduced the significance of the results. EAE onset expression is highly dependent on a variety of aspects, from species, age and gender of the animals to housing conditions, stress and diet[36]. Therefore, most of these aspects were followed accordingly to what is described in previous studies. In accordance to what has been previously assessed on gender influence on EAE expression, female C57BL/6 mice were used to induce the EAE model, since females are more prone to develop severe EAE pathology, by having stronger Th1-mediated immune responses[110]. Furthermore, it has been described that active induction of female C57BL/6 mice strain with MOG_{35-55} antigen efficiently activates T and B cell-mediated autoimmune response, leading to neurological impairments and demyelination lesions very similar to lesions observed in MS patients with chronic non-remitting form[37,43,111]. However, our results on CS development showed a partial recovery of the phenotype in some of the individuals, meaning that chronic non-remitting MS model was not developed. Overall, EAE model development in EAE VEH and EAE CGS groups was quite similar, with EAE onset of the EAE VEH at day 17 p.i., reaching the peak 4 days after, while EAE CGS group onset was at day 19 p.i., reaching the peak also 4 days after. In both groups, onset was delayed, comparatively to the 9-14 days p.i. previously described[36,44].

Animal stress might be one of the major impact factors for the low incidence and severity of the EAE model. On the day following the induction protocol, animals were subjected to a very demanding BrdU protocol, which, in turn, was followed by the micro-osmotic pump implantation surgery, on the following day. These procedures require an intensive handling and restrain of the animals, which may increase the distress of the animals, causing the delay observed on EAE onset and its low severity. Moreover, the fact that animals were individually housed to allow a full post-surgery recovery may also be a stress factor due to lack of social contact, as mice are a social interactive species[112]. Concurrently, housing acclimatization was also altered on day 7 p.i, with animals being moved from an SPF facility to a VAF area. This change was due to previous assessments[113,114] on how environment may influence EAE pathogenic autoimmune response, where it was observed that animals induced in a SPF environment displayed a more severe course of EAE onset when compared with animals induced in conventional housing or in a germ-free environment. However, animals had to be changed on day 7 p.i. so that behavioural tests could be performed. Furthermore, although female mice have been described to express more aggravated EAE pathogenesis, the hormonal cycle stage in which the animals were induced could also have had some influence on the model progression. In fact, Voskuhl et al., have

observed that, during pregnancy, as estradiol and progesterone levels are increased, there was an amelioration in EAE progression[115]. Moreover, ovariectomized EAE mice treated with a medium dosage of estrogen, similar to pregnancy levels, showed an inhibition in the disease progression[116]. However, in a different study, ovariectomized EAE mice and sham EAE females showed no significant differences in the disease progression, implying that female sex hormones may have a minor influence in EAE progression[115]. Thus, if the animals were induced during a stage of the hormonal cycle in which these hormone levels were increased, this could have affected EAE clinical course. For a proper initiation of the autoimmune response against MOG_{35-55} antigen, PTX is required to be functional so as to increase BBB permeability, facilitating pathogenic T cells migration, thus exacerbating the inflammatory response[41,117]. PTX dosage was adjusted to optimize its potency, accordingly to the Hooke Kit's PTX dose adjustment methodology[44], considering stress augmentation due to the osmotic pump implantation and BrdU administration. Moreover, PTX was administered i.p. to reduce procedure stress. Yet, PTX dosage may still not be the most adequate which may interfere with MOG_{35-55} immunization activation in the CNS. In fact, although many studies have confirmed that PTX is essential for MOG_{35-55} induction in C57BL/6 mice[36,41,118], Yin et al. have presented data observing that PTX has a protective effect in EAE, by reducing lymphocyte infiltration, decreasing EAE clinical signs[119]. Ultimately, PTX malfunctioning or inactivation could have annihilated its role in the model induction. Moreover, due to the pump implantation procedure, MOG_{35-55} injection site was performed not dorsally but ventrally which is accessible to the animal who involuntarily can rupture the emulsion site, causing emulsion leakage, thus, tarnishing the antigen administration.

Importantly, the low incidence in EAE CGS group and lower CS might reflect a putative protective role of $A_{2A}R$ agonist. Several studies have reported that CGS21680 has an ambiguous role in the inflammatory response under EAE conditions, by both enhancing migration of inflammatory lymphocytes into the CNS[63] and diminishing the expression of pro-inflammatory cytokines[75], thus attenuating EAE expression. Additionally, in previous work performed in our lab, it was observed that $A_{2A}R$ activation promoted OPCs differentiation and maturation into myelinating OLGs from SVZ NSCs[92]. Furthermore, Ingwersen et al. have compared prophylactic CGS21680 treatment with CGS21680 treatment at the peak and have concluded that preventive CGS treatment causes a delay in the disease onset and a prevention of the disease symptoms[120]. Therefore, we expected that CGS icv administration would have had some effect on EAE phenotype expression. However, no significant differences are observed when comparing EAE VEH group clinical course with EAE CGS group. EAE CGS animals presented a two-days delay of the EAE onset comparatively to EAE VEH animals with one animal with a similar clinical course while the other with a lower CS. Due to the low EAE model incidence and low experimental *n*, it was not possible to conclusively assess the role of the $A_{2A}R$ agonist in the EAE clinical course. Additionally, the CGS21680 concentration may not have been enough to cause any major impacts in the lateral ventricle environment, especially, under EAE neuroinflammatory conditions.

EAE progression monitoring was complemented with a battery of behavioural tests, which included OF, PT and RR, to evaluate the locomotor and exploratory activity and to assess whether $A_{2A}R$ agonist treated-animals would show any differences regarding vehicle treated animals. Previous studies support that some of these behavioural parameters, namely, travelled distance in OF[106], RR latency ($t_{fall,}$ in our

analysis)[121], or $t_{descend}$ in PT[102], establish a good correlation of motor and balance impairments with EAE clinical course. As mentioned, two set of analysis were performed. Only when we analysed separately the animals with high CS from the animals with CS=0 we could correlate EAE CS severity and behavioural performance parameters. Overall, in all 3 behavioural assays, it was observable that EAE animals with higher CS presented motor and balance impairments thus having a negative impact on their performance in the test. However, results did not provide any conclusions on the influence that CGS21680 administration might have had in motor and exploratory abilities, as results from the EAE CGS CS>1 group did not achieve significant variations when compared with the EAE VEH CS>1 group. Once again, this lack of significance and conclusiveness in behavioural results is due to a low incidence obtained in the model, leading to a low experimental *n* in both groups.

MBP and PLP protein levels, the most abundant proteins of the myelin sheath and highly responsible for its compactness[108,109], were assessed by western blot techniques to study de- and remyelination, particularly in the cortex, striatum, CC and SVZ. It has been described that under EAE inflammatory and demyelinating conditions, these proteins are highly degraded because of myelin damage and OLGs death[122]. Hence, this evaluation would not only allow an evaluation of myelin levels but would also serve as an indirect assessment of OLGs myelinating activity, as these myelin proteins are markers of mature myelinating OLGs[50]. Overall, no significant differences were observed when comparing EAE VEH and EAE CGS groups, both in MBP and PLP levels. Moreover, both EAE VEH and EAE CGS groups with CS>1 did not present a significant decrease comparatively to EAE VEH and EAE CGS with CS=0, respectively. Thus, it was not possible to establish a correlation between higher CS and degradation rates of MBP and PLP, contrarily to Bernardes et al. observation of myelin proteins degradation in EAE animals[122]. Nevertheless, a tendency is observed in PLP levels of cortical lysates samples, in which EAE CGS CS>1 animals presented much lower PLP levels than EAE VEH CS>1, suggesting that CGS 21680, contrary to what we expected, might inhibit the remyelinating response. Coppi and colleagues have shown that $A_{2A}R$ had an inhibiting effect in cultured OPCs maturation, which may be the cause behind this decrease in PLP expression[70]. Moreover, EAE VEH with CS>1 presented higher PLP levels than CTRL or EAE VEH animals with CS=0. This may result from an intensified remyelinating response to compensate EAE pathogenic lesions. Yet again, sample size is not significant to make any conclusion.

Concurrently, immunohistochemical and histological assays did not provide any additional information regarding myelin levels in different conditions. Regarding CC myelination, immunohistochemistry for MBP staining and LFB results are quite coherent. In both tests, in every condition, this area is presented as highly myelinated, with no relevant CC area reduction between conditions in IHC and with an intense blue colour in LFB, indicative of high myelin levels. Regarding LFB assay, the intense blue colour visible in the CC area could be a sign of an intense remyelinating response, as this is one of the most affected areas by demyelination. Picard-Riera et al. have shown that OPCs migrate from the SVZ to the CC, restoring myelin levels[60].

Regarding NF-κB signaling pathway, results were also not very informative. NF-κB activation has been described to enhance the inflammatory response under MS or EAE pathogenesis[77,123]. It has also been described that, in spinal cord injured animals, the inhibition of NF-κB transduction in astrocytes promoted oligodendrogenesis in this inflammatory environment[124]. Furthermore, $A_{2A}R$ role has an

inhibitory role in the activation of NF-κB[67], suppressing inflammation[76]. However, in the four brain areas analysed it was not possible to observe any changes in this pathway. Variations between conditions are not prominent, despite a slight increase observed in pNF-κB protein levels in cortical samples of EAE CGS CS>1 animals. This increase might be associated with EAE pathogenic inflammation. Regarding pIκB protein levels, it was not possible to establish a correlation with pNF-κB protein levels, besides a similar tendency in striatum and SVZ samples. Hence, sample size should be increased to better assess these hypotheses.

In regard to ERK1/2 pathway activation, Morello et al. have shown that $A_{2A}R$ activate this signaling pathway[78]. In addition, Maricich et al. have demonstrated that this signaling pathway is activated as OPCs differentiate into mature myelinating OLGs[125]. Moreover, in MS and EAE conditions, although inflammatory T cells and macrophages expressed MAPK/ERK phosphorylation, this pathway activation has not been described to cause a major impact in the diseases clinical course[84]. Regarding pERK1/2 protein levels no changes were observed between EAE CGS and EAE VEH. However, in cortical and CC samples an increase in pERK1/2 was seen in EAE CGS CS>1, possibly related with mature myelinating OLGs activity in response to demyelination. Contrarily, in both SVZ and striatum, this tendency is not observed. Thus, once again, sample size and low EAE incidence were not sufficient to make any conclusions on the role that CGS21680 might have in the activation of the ERK1/2 pathway under EAE pathological conditions.

Taken together, the low incidence and severity of the EAE model were the main limiting factors of this work. Consequently, a small sample size of EAE CGS and EAE VEH conditions did not allow a conclusive analysis of the $A_{2A}R$ role in EAE phenotype ablation or its effects in OLGs remyelinating activity.

5. Conclusion and Future Perspectives

The aim of this project was to evaluate the role of $A_{2A}R$ in modulating the production of OLGs, thus inducing myelination under EAE pathogenic conditions. To do so, 10 female C57BL/6 ten-weeks old were immunized with an emulsion of MOG_{35-55} in CFA and injected with PTX to induce the EAE model, the most widely used animal model of MS. EAE animals were submitted to a stereotaxic surgery to implant a micro-osmotic pump to locally administer in the right lateral ventricle an $A_{2A}R$ agonist solution or the vehicle solution for 26 days. Behavioural performance of EAE animals and molecular and cellular analysis, were compared with a naïve control group.

Overall, EAE model induction was not successful, with only an incidence of 40% in the EAE VEH group, which constrained the significance of the results. EAE animals showed impaired performance in behavioral tests as EAE phenotype was progressing. However, no relevant differences were observed in EAE CGS when compared with EAE VEH animals. Moreover, no tendency for changes was observed at a molecular level, regarding either the NF-κB or the MAPK/ERK(1/2) signaling pathways. Regarding demyelination, both LFB and MBP immunohistochemical staining showed that myelin amounts in the EAE brain, for both EAE VEH and EAE CGS animals, were similar to CTRL animals. The major drawback of this work was the low incidence of the EAE model induction that, consequently, reduced sample size of animals expressing EAE phenotype, limiting statistical analysis assessments and EAE phenotype correlations with behavioural performances or results from molecular assays. Moreover, EAE severity was rather mild, never surpassing a CS of 2-3, which may have hindered EAE pathological symptoms intensity, namely inflammation and demyelination.

In the future, some troubleshooting approaches should be performed as an attempt to optimize EAE model induction. For instance, MOG_{35-55} injection site could be performed on the lower dorsal flank to avoid emulsion leakage. Furthermore, it would be of further interest to perform a permeability assay of the BBB[126], to evaluate PTX ability to disrupt the BBB and adjust its optimal dose regarding our experimental protocol. Moreover, to assess whether animal stress induced by the intense *in vivo* protocol, i.e., the BrdU administration protocol and the osmotic pump implantation surgery, it would be appropriate to immunize the animals and avoid any stress-inducing procedures, leaving the animals at rest, for, at least, two weeks. Besides improvements on the EAE induction protocol, our future work will be focused on increasing sample size in order to perform supplementary molecular and cellular analysis, that could sustain our hypothesis. BrdU staining should be analysed to compare oligodendrogenesis and cell proliferation under $A_{2A}R$ activation in EAE conditions, combined with IHC assays of OLGs lineage markers, as Olig2, GalC, or NG2, to thoroughly assess oligodendrogenesis in the brain. Furthermore, additional $A_{2A}R$ signaling pathways could be assessed to further evaluate the role of this receptor in MS. For instance, assessing JNK/MAPK signaling pathway activation along with phospho-JNK expression in OLGs would be an exciting approach to assess CGS21680 protective role in neuroinflammation, particularly in OLGs, as described by Genovese and colleagues[89]. Altogether, these assays could provide useful data to optimize $A_{2A}R$ concentration. Moreover, LFB assays on spinal cord

samples would complement our studies on demyelination and endogenous remyelination phenomena in the CNS.

In sum, further assays are required to corroborate the hypothesis presented in this work, in order to unequivocally consider $A_{2A}R$ a promising approach to reinforce oligodendrogenesis under demyelinating and neuroinflammatory conditions towards the development of regenerative therapies in MS.

6. References

1. Leray, E., Moreau, T., Fromont, A. & Edan, G. Epidemiology of multiple sclerosis. *Rev. Neurol. (Paris).* **172,** 3–13 (2016).

2. Msif. Atlas of MS 2013: Mapping Multiple Sclerosis Around the World. *Mult. Scler. Int. Fed.* 1–28 (2013). doi:10.1093/brain/awm236

3. Goldenberg M., M. Multiple Sclerosis. *Pathy's Princ. Pract. Geriatr. Med. Fifth Ed.* **37,** 175–184 (2012).

4. Compston, A. & Coles, A. Multiple sclerosis. *Lancet* **372,** 1502–1517 (2008).

5. Loma, I. & Heyman, R. Multiple Sclerosis: Pathogenesis and Treatment. *Curr. Neuropharmacol.* **9,** 409–416 (2011).

6. Koch, M. W., Metz, L. M. & Kovalchuk, O. Epigenetic changes in patients with multiple sclerosis. *Nat. Rev. Neurol.* **9,** 35–43 (2013).

7. Wu F., G. & Alvarez, E. The immuno-pathophysiology of multiple sclerosis. *Neurol Clin* **1,** 257–278 (2011).

8. Mólnar, P. The Central Nervous System. in *Pathology Secrets* 448–476 (Mosby, 2009). doi:10.1016/B978-0-323-05594-9.00022-2

9. Popescu, B. F. G. & Lucchinetti, C. F. Neuropathology of multiple sclerosis. *Mult. Scler. A Mech. View* 181–200 (2015). doi:10.1016/B978-0-12-800763-1.00009-9

10. Miron, V. E., Kuhlmann, T. & Antel Jack P., J. P. Cells of the oligodendroglial lineage, myelination, and remyelination. *Biochim. Biophys. Acta - Mol. Basis Dis.* **1812,** 184–193 (2011).

11. Lassmann, H. Pathology and disease mechanisms in different stages of multiple sclerosis. *J. Neurol. Sci.* **333,** 1–4 (2013).

12. Steinman, L. & Zamvil, S. Transcriptional analysis of targets in multiple sclerosis. *Nat. Rev. Immunol.* **3,** 483–492 (2003).

13. Franklin, R. J. M. & Ffrench-Constant, C. Remyelination in the CNS: From biology to therapy. *Nat. Rev. Neurosci.* **9,** 839–855 (2008).

14. Hemmer, B., Archelos, J. J. & Hartung, H. P. New concepts in the immunopathogenesis of multiple sclerosis. *Nat. Rev. Neurosci.* **3,** 291–301 (2002).

15. Michailidou, I., de Vries, H. E., Hol, E. M. & van Strien, M. E. Activation of endogenous neural stem cells for multiple sclerosis therapy. *Front. Neurosci.* **9,** 1–8 (2015).

16. Prineas, J. W., Barnard, R. O., Kwon, E. E., Sharer, L. R. & Cho, E. -S. Multiple sclerosis: Remyelination of nascent lesions: Remyelination of nascent lesions. *Ann. Neurol.* **33,** 137–151

(1993).

17. Scolding, N. *et al.* Oligodendrocyte progenitors are present in the normal adult human CNS and in the lesions of multiple sclerosis. *Brain* **121 (Pt 1,** 2221–2228 (1998).

18. Goldschmidt, T., Antel, J., König, F. B., Brück, W. & Kuhlmann, T. Remyelination capacity of the MS brain decreases with disease chronicity. *Neurology* **72,** 1914–1921 (2009).

19. How is MS Treated? *Multiple Sclerosis Trust* Available at: https://www.mstrust.org.uk/about-ms/how-ms-treated. (Accessed: 15th August 2018)

20. Wingerchuk, D. M. & Carter, J. L. Multiple sclerosis: Current and emerging disease-modifying therapies and treatment strategies. *Mayo Clin. Proc.* **89,** 225–240 (2014).

21. Xie, C., Liu, Y.-Q., Guan, Y.-T. & Zhang, G.-X. Induced Stem Cells as a Novel Multiple Sclerosis Therapy. *Curr. Stem Cell Res. Ther.* **11,** 313–320 (2016).

22. Shroff, G. A review on stem cell therapy for multiple sclerosis: Special focus on human embryonic stem cells. *Stem Cells Cloning Adv. Appl.* **11,** 1–11 (2018).

23. Sarkar, P., Rice, C. M. & Scolding, N. J. Cell Therapy for Multiple Sclerosis. *CNS Drugs* **31,** 453–469 (2017).

24. Radaelli, M. *et al.* Autologous bone marrow transplantation for the treatment of multiple sclerosis. *Curr. Neurol. Neurosci. Rep.* **14,** (2014).

25. Reekmans, K. P. *et al.* Clinical potential of intravenous neural stem cell delivery for treatment of neuroinflammatory disease in mice? *Cell Transplant.* **20,** 851–869 (2011).

26. Gerdoni, E. *et al.* Mesenchymal stem cells effectively modulate pathogenic immune response in experimental autoimmune encephalomyelitis. *Ann. Neurol.* **61,** 219–227 (2007).

27. Douvaras, P. *et al.* Efficient generation of myelinating oligodendrocytes from primary progressive multiple sclerosis patients by induced pluripotent stem cells. *Stem Cell Reports* **3,** 250–259 (2014).

28. Harlow, D. E., Honce, J. M. & Miravalle, A. A. Remyelination Therapy in Multiple Sclerosis. *Front Neurol* **6,** 257 (2015).

29. Fancy, S. P. J. *et al.* Dysregulation of the Wnt pathway inhibits timely myelination and remyelination in the mammalian CNS. *Genes Dev.* **23,** 1571–1585 (2009).

30. Zhang, Y. *et al.* Notch1 signaling plays a role in regulating precursor differentiation during CNS remyelination. *Proc. Natl. Acad. Sci.* **106,** 19162–19167 (2009).

31. Fyffe-maricich, S. L., Karlo, J. C., Landreth, G. E. & Miller, R. H. The ERK2 Mitogen-Activated Protein Kinase Regulates the Timing of Oligodendrocyte Differentiation. **31,** 843–850 (2013).

32. Bjelobaba, I., Begovic-Kupresanin, V., Pekovic, S. & Lavrnja, I. Animal models of multiple

sclerosis: Focus on experimental autoimmune encephalomyelitis. *J. Neurosci. Res.* **96,** 1021–1042 (2018).

33. Matsushima, G. K. & Morell, P. The Neurotoxicant, Cuprizone, as a Model to Study Demyelination and Remyelination in the Central Nervous System. *Brain Pathol.* **11,** 107–116 (2006).

34. Procaccini, C., De Rosa, V., Pucino, V., Formisano, L. & Matarese, G. Animal models of Multiple Sclerosis. *Eur. J. Pharmacol.* **759,** 182–191 (2015).

35. Koritschoner, R. S. & Schweinburg, F. Induktion von Paralyse und Rückenmarksentzündung durch Immunisierung von Kaninchen mit menschlichem Rückenmarksgewebe. *Z. Immunitätsf. Exp. Ther.* 217–283 (1925).

36. Stromnes, I. M. & Goverman, J. M. Active induction of experimental allergic encephalomyelitis. *Nat. Protoc.* **1,** 1810–1819 (2006).

37. Recks, M. S. *et al.* Early axonal damage and progressive myelin pathology define the kinetics of CNS histopathology in a mouse model of multiple sclerosis. *Clin. Immunol.* **149,** 32–45 (2013).

38. Stromnes, I. M. & Goverman, J. M. Passive induction of experimental allergic encephalomyelitis. *Nat. Protoc.* **1,** 1952–1960 (2006).

39. Linnington, C., Webb, M. & Woodhams, P. L. A novel myelin-associated glycoprotein defined by a mouse monoclonal antibody. *J. Neuroimmunol.* (1984). doi:10.1016/0165-5728(84)90064-X

40. Herrero-Herranz, E., Pardo, L. A., Gold, R. & Linker, R. A. Pattern of axonal injury in murine myelin oligodendrocyte glycoprotein induced experimental autoimmune encephalomyelitis: Implications for multiple sclerosis. *Neurobiol. Dis.* **30,** 162–173 (2008).

41. Miller, S. D., Karpus, W. J. & Davidson, T. S. Experimental Autoimmune Encephalomyelitis in the Mouse. *Curr Protoc Immunol.* 1–26 (2007). doi:10.1002/0471142735.im1501s77.Experimental

42. Constantinescu, C. S., Farooqi, N., O'Brien, K. & Gran, B. Experimental autoimmune encephalomyelitis (EAE) as a model for multiple sclerosis (MS). *Br. J. Pharmacol.* **164,** 1079–1106 (2011).

43. 't Hart, B. A., Gran, B. & Weissert, R. EAE: Imperfect but useful models of multiple sclerosis. *Trends Mol. Med.* **17,** 119–125 (2011).

44. Laboratories, H. EAE Induction by Active Immunization in C57BL/6 Mice. **2,** 1–20 (2014).

45. Ming, G. li & Song, H. Adult Neurogenesis in the Mammalian Brain: Significant Answers and Significant Questions. *Neuron* **70,** 687–702 (2011).

46. Borsini, A., Zunszain, P. A., Thuret, S. & Pariante, C. M. The role of inflammatory cytokines as key modulators of neurogenesis. *Trends Neurosci.* **38,** 145–157 (2015).

47. Kojima, T. *et al.* Subventricular zone-derived neural progenitor cells migrate along a blood vessel

scaffold toward the post-stroke striatum. *Stem Cells* (2010). doi:10.1002/stem.306

48. Gould, E. How widespread is adult neurogenesis in mammals? *Nature Reviews Neuroscience* (2007). doi:10.1038/nrn2147

49. Chang, A. *et al.* Neurogenesis in the chronic lesions of multiple sclerosis. *Brain* **131,** 2366–2375 (2008).

50. Waly, B. El, Macchi, M., Cayre, M. & Durbec, P. Oligodendrogenesis in the normal and pathological central nervous system. *Front. Neurosci.* **8,** 1–22 (2014).

51. Grade, S., Bernardino, L. & Malva, J. O. Oligodendrogenesis from neural stem cells: Perspectives for remyelinating strategies. *Int. J. Dev. Neurosci.* **31,** 692–700 (2013).

52. Dawson, M. R. L., Levine, J. M. & Reynolds, R. NG2-expressing cells in the central nervous system: Are they oligodendroglial progenitors? *Journal of Neuroscience Research* (2000). doi:10.1002/1097-4547(20000901)61:5<471::AID-JNR1>3.0.CO;2-N

53. Armada-Moreira, A., Ribeiro, F., Sebastião, A. & Xapelli, S. Neuroinflammatory modulators of oligodendrogenesis. *Neuroimmunol. Neuroinflammation* **2,** 263 (2015).

54. Menn, B. *et al.* Origin of Oligodendrocytes in the Subventricular Zone of the Adult Brain. *J. Neurosci.* **26,** 7907–7918 (2006).

55. Ortega, F. *et al.* Oligodendrogliogenic and neurogenic adult subependymal zone neural stem cells constitute distinct lineages and exhibit differential responsiveness to Wnt signalling. *Nat. Cell Biol.* (2013). doi:10.1038/ncb2736

56. Traiffort, E., Zakaria, M., Laouarem, Y. & Ferent, J. Hedgehog: A Key Signaling in the Development of the Oligodendrocyte Lineage. *J. Dev. Biol.* **4,** 28 (2016).

57. Colak, D. *et al.* Adult Neurogenesis Requires Smad4-Mediated Bone Morphogenic Protein Signaling in Stem Cells. *J. Neurosci.* (2008). doi:10.1523/JNEUROSCI.4374-07.2008

58. Kotter, M. R., Setzu, A., Sim, F. J., Van Rooijen, N. & Franklin, R. J. M. Macrophage depletion impairs oligodendrocyte remyelination following lysolecithin-induced demyelination. *Glia* (2001). doi:10.1002/glia.1085

59. Li, J. S. & Yao, Z. X. MicroRNAs: Novel regulators of oligodendrocyte differentiation and potential therapeutic targets in demyelination-related diseases. *Mol. Neurobiol.* (2012). doi:10.1007/s12035-011-8231-z

60. Picard-Riera, N. *et al.* Experimental autoimmune encephalomyelitis mobilizes neural progenitors from the subventricular zone to undergo oligodendrogenesis in adult mice. *Proc. Natl. Acad. Sci.* **99,** 13211–13216 (2002).

61. Nait-Oumesmar, B. *et al.* Activation of the subventricular zone in multiple sclerosis: Evidence for early glial progenitors. *Proc. Natl. Acad. Sci.* **104,** 4694–4699 (2007).

62. Du, C. & Xie, X. G protein-coupled receptors as therapeutic targets for multiple sclerosis. *Cell Res.* **22,** 1108–1128 (2012).

63. Mills, J. H., Kim, D.-G., Krenz, A., Chen, J.-F. & Bynoe, M. S. A2A Adenosine Receptor Signaling in Lymphocytes and the Central Nervous System Regulates Inflammation during Experimental Autoimmune Encephalomyelitis. *J. Immunol.* **188,** 5713–5722 (2012).

64. Ribeiro, J. A., Sebastião, A. M. & De Mendonça, A. Adenosine receptors in the nervous system: Pathophysiological implications. *Prog. Neurobiol.* **68,** 377–392 (2002).

65. Rajasundaram, S. Adenosine A2A Receptor Signaling in the Immunopathogenesis of Experimental Autoimmune Encephalomyelitis. *Front. Immunol.* **9,** (2018).

66. Cekic, C. & Linden, J. Purinergic regulation of the immune system. *Nature Reviews Immunology* (2016). doi:10.1038/nri.2016.4

67. Fredholm, B. B., Chern, Y., Franco, R. & Sitkovsky, M. Aspects of the general biology of adenosine A2Asignaling. *Prog. Neurobiol.* **83,** 263–276 (2007).

68. Weaver, D. R. A(2A) adenosine receptor gene-expression in developing rat brain. *Mol Brain Res* (1993).

69. Othman, T., Yan, H. & Rivkees, S. A. Oligodendrocytes Express Functional A1 Adenosine Receptors That Stimulate Cellular Migration. *Glia* **44,** 166–172 (2003).

70. Coppi, E., Cellai, L., Maraula, G., Pugliese, A. M. & Pedata, F. Adenosine A2Areceptors inhibit delayed rectifier potassium currents and cell differentiation in primary purified oligodendrocyte cultures. *Neuropharmacology* **73,** 301–310 (2013).

71. Coppi, E. *et al.* Role of adenosine in oligodendrocyte precursor maturation. *Front. Cell. Neurosci.* **9,** 1–8 (2015).

72. Cekic, C. & Linden, J. Purinergic regulation of the immune system. *Nat. Rev. Immunol.* **16,** 177–192 (2016).

73. Mills, J. H. *et al.* CD73 is required for efficient entry of lymphocytes into the central nervous system during experimental autoimmune encephalomyelitis. *Proc. Natl. Acad. Sci.* (2008). doi:10.1073/pnas.0711175105

74. Mayne, M., Shepel, P. N., Jiang, Y., Geiger, J. D. & Power, C. Dysregulation of adenosine A1receptor-mediated cytokine expression in peripheral blood mononuclear cells from multiple sclerosis patients. *Ann. Neurol.* (1999). doi:10.1002/1531-8249(199905)45:5<633::AID-ANA12>3.0.CO;2-X

75. Liu, Y. *et al.* Activation of the adenosine A2A receptor attenuates experimental autoimmune encephalomyelitis and is associated with increased intracellular calcium levels. *Neuroscience* **330,** 150–161 (2016).

76. Milne R., G. & Palmer M., T. Anti-inflammatory and Immunosuppressive effects of A2A Receptors. *Int. Geosci. Remote Sens. Symp.* 4788–4791 (2010). doi:10.1100/tsw.2011.22

77. Yue, Y., Stone, S. & Lin, W. Role of nuclear factor κB in multiple sclerosis and experimental autoimmune encephalomyelitis. *Neural Regen. Res.* **13,** 1507 (2018).

78. Morello, S. & Sorrentino, R. Adenosine A2A receptor agonists as regulators of inflammation : pharmacology and therapeutic opportunities Adenosine A2a receptor agonists as regulators of inflammation : pharmacology and therapeutic opportunities. (2009). doi:10.2147/JRLCR.S4710

79. Hayden, M. S. & Ghosh, S. Shared Principles in NF-κB Signaling. *Cell* **132,** 344–362 (2008).

80. Lawrence, T. The nuclear factor NF-kappaB pathway in inflammation. *Cold Spring Harb. Perspect. Biol.* **1,** 1–10 (2009).

81. Kaltschmidth, B. & Kaltschmidt, C. Nf-kB in the Nervous System. *Clin. Infect. Dis.* **27,** 256–258 (1998).

82. Stone, S. *et al.* NF-κB Activation Protects Oligodendrocytes against Inflammation. *J. Neurosci.* **37,** 9332–9344 (2017).

83. Zhang, Y. *et al.* Nuclear factor kappa B signaling initiates early differentiation of neural stem cells. *Stem Cells* **30,** 510–524 (2012).

84. Birkner, K. *et al.* The role of ERK signaling in experimental autoimmune encephalomyelitis. *Int. J. Mol. Sci.* **18,** (2017).

85. Zhang, W. & Liu, H. T. MAPK signal pathways in the regulation of cell proliferation in mammalian cells. **12,** 9–18 (2002).

86. Cargnello, M. & Roux P., P. Activation and Function of the MAPKs and Their Substrates, the MAPK-Activated Protein Kinases. *Microbiol. Mol. Biol. Rev.* **64,** 65–67 (2011).

87. Seger, R. & Krebs, E. G. Signaling Cascade. *Faseb J.* **9,** 726–735 (1995).

88. Pedram, A., Razandi, M. & Levin, E. R. Extracellular signal-regulated protein kinase/jun kinase cross-talk underlies vascular endothelial cell growth factor-induced endothelial cell proliferation. *J. Biol. Chem.* **273,** 26722–26728 (1998).

89. Genovese, T. *et al.* The selective adenosine A2A receptor agonist CGS 21680 reduces JNK MAPK activation in oligodendrocytes in injured spinal cord. *Shock* **32,** 578–585 (2009).

90. Schulte, G. & Fredholm, B. B. Signalling from adenosine receptors to mitogen-activated protein kinases. *Cell. Signal.* **15,** 813–827 (2003).

91. Ishii, A., Fyffe-Maricich, S. L., Furusho, M., Miller, R. H. & Bansal, R. ERK1/ERK2 MAPK signaling is required to increase myelin thickness independent of oligodendrocyte differentiation and initiation of myelination. **6,** 790–795 (2015).

92. Armada-Moreira, A. & Xapelli, S. Exploring the modulatory role of A2A receptors in oligodendrogenesis derived from neural stem/progenitor cells of the subventricular zone. (Faculdade de Medicina - Universidade de Lisboa, 2015).

93. Taupin, P. BrdU immunohistochemistry for studying adult neurogenesis: Paradigms, pitfalls, limitations, and validation. *Brain Res. Rev.* **53,** 198–214 (2007).

94. Alberts, B. *et al.* 2014 ASCB/IFCB Meeting abstracts. *Mol. Biol. Cell* **25,** 3987–3987 (2014).

95. Ialenti, A., Caiazzo, E., Morello, S., Carnuccio, R. & Cicala, C. Adenosine A_{2A} Receptor Agonist, 2- *p* -(2-Carboxyethyl)phenethylamino-5′- *N* -ethylcarboxamidoadenosine Hydrochloride Hydrate, Inhibits Inflammation and Increases Fibroblast Growth Factor-2 Tissue Expression in Carrageenan-Induced . *J. Pharmacol. Exp. Ther.* **364,** 221–228 (2018).

96. Theeuwes, F. & Yum, S. I. Principles of the design and operation of generic osmotic pumps for the delivery of semisolid or liquid drug formulations. *Annals of Biomedical Engineering* **4,** 343–353 (1976).

97. Durect Corporation. Micro - Osmotic Pump Model 1004 Instructions and Specification Sheet. 1–2 (2016).

98. Paxinos, G. & Franklin, K. B. J. *The Mouse Brain in Stereotaxic Coordinates*. *Academic Press* (2004). doi:10.1016/S0306-4530(03)00088-X

99. Chora, Â. A. *et al.* Heme oxygenase–1 and carbon monoxide suppress autoimmune neuroinflammation. **117,** 3–12 (2007).

100. Balkaya, M., Kröber, J. M., Rex, A. & Endres, M. Assessing post-stroke behavior in mouse models of focal ischemia. *J. Cereb. Blood Flow Metab.* **33,** 330–338 (2013).

101. Lu, J. *et al.* Pain in experimental autoimmune encephalitis: A comparative study between different mouse models. *J. Neuroinflammation* **9,** 1 (2012).

102. Matsuura, K., Kabuto, H., Makino, H. & Ogawa, N. Pole test is a useful method for evaluating the mouse movement disorder caused by striatal dopamine depletion. *J. Neurosci. Methods* **73,** 45–48 (1997).

103. Mandolesi, G. *et al.* Synaptopathy connects inflammation and neurodegeneration in multiple sclerosis. *Nat. Rev. Neurol.* **11,** 711–724 (2015).

104. Gilli, F., Royce, D. B. & Pachner, A. R. Measuring Progressive Neurological Disability in a Mouse Model of Multiple Sclerosis. *J. Vis. Exp.* 1–8 (2016). doi:10.3791/54616

105. van den Berg, R., Laman, J. D., van Meurs, M., Hintzen, R. Q. & Hoogenraad, C. C. Rotarod motor performance and advanced spinal cord lesion image analysis refine assessment of neurodegeneration in experimental autoimmune encephalomyelitis. *J. Neurosci. Methods* **262,** 66–76 (2016).

106. Takemiya, T. & Takeuchi, C. Traveled Distance Is a Sensitive and Accurate Marker of Motor Dysfunction in a Mouse Model of Multiple Sclerosis. *ISRN Neurosci.* **2013,** 1–4 (2013).

107. Heneka, M. T. *et al.* The heat shock response reduces myelin oligodendrocyte glycoprotein-induced experimental autoimmune encephalomyelitis in mice. *J. Neurochem.* **77,** 568–579 (2001).

108. Boison, D., Büssow, H., D'Urso, D., Müller, H.-W. & Stoffel, W. Adhesive properties of proteolipid protein are responsible for the compaction of CNS myelin sheaths. *J. Neurosci.* **15,** 5502–13 (1995).

109. Weil, M. T. *et al.* Loss of Myelin Basic Protein Function Triggers Myelin Breakdown in Models of Demyelinating Diseases. *Cell Rep.* **16,** 314–322 (2016).

110. Massella, A. *et al.* Gender effect on neurodegeneration and myelin markers in an animal model for multiple sclerosis. *BMC Neurosci.* **13,** (2012).

111. Bernard, C. C. A. *et al.* Myelin oligodendrocyte glycoprotein: A novel candidate autoantigen in multiple sclerosis. *J. Mol. Med.* **75,** 77–88 (1997).

112. Kappel, S., Hawkins, P. & Mendl, M. T. To group or not to group? Good practice for housing male laboratory mice. *Animals* **7,** 1–25 (2017).

113. Lee, Y. K., Menezes, J. S., Umesaki, Y. & Mazmanian, S. K. Proinflammatory T-cell responses to gut microbiota promote experimental autoimmune encephalomyelitis. *Proc. Natl. Acad. Sci.* **108,** 4615–4622 (2011).

114. Arndt, A. *et al.* Conventional housing conditions attenuate the development of experimental autoimmune encephalomyelitis. *PLoS One* **9,** (2014).

115. Voskuhl, R. R. & Palaszynski, K. Sex hormones in experimental autoimmune encephalomyelitis: Implications for multiple sclerosis. *Neuroscientist* **7,** 258–270 (2001).

116. Haghmorad, D. *et al.* Medium-dose estrogen ameliorates experimental autoimmune encephalomyelitis in ovariectomized mice. *J. Immunotoxicol.* **13,** 885–896 (2016).

117. Bennett, J. *et al.* Blood-brain barrier disruption and enhanced vascular permeability in the multiple sclerosis model EAE. *J. Neuroimmunol.* **229,** 180–191 (2010).

118. Bettelli, E. *et al.* Myelin Oligodendrocyte Glycoprotein–specific T Cell Receptor Transgenic Mice Develop Spontaneous Autoimmune Optic Neuritis. *J. Exp. Med.* **197,** 1073–1081 (2003).

119. Yin, J. X. *et al.* Pertussis toxin modulates microglia and T cell profile to protect experimental autoimmune encephalomyelitis. *Neuropharmacology* **81,** 1–5 (2014).

120. Ingwersen, J. *et al.* Dual roles of the adenosine A2a receptor in autoimmune neuroinflammation. *J. Neuroinflammation* **13,** (2016).

121. Sands, S. A. *et al.* The effect of omeprazole on the development of experimental autoimmune encephalomyelitis in C57BL/6J and SJL/J mice. *BMC Res. Notes* **7,** 1–11 (2014).

122. Bernardes, D. *et al.* Prior regular exercise improves clinical outcome and reduces demyelination and axonal injury in experimental autoimmune encephalomyelitis. *J. Neurochem.* **136,** 63–73 (2016).

123. Leibowitz, S. M. & Yan, J. NF-κB Pathways in the Pathogenesis of Multiple Sclerosis and the Therapeutic Implications. *Front. Mol. Neurosci.* **9,** 1–23 (2016).

124. Bracchi-Ricard, V. *et al.* Inhibition of astroglial NF-kappaB enhances oligodendrogenesis following spinal cord injury. *J. Neuroinflammation* **10,** 1 (2013).

125. Jeffries, M. A. *et al.* ERK1/2 Activation in Preexisting Oligodendrocytes of Adult Mice Drives New Myelin Synthesis and Enhanced CNS Function. *J. Neurosci.* **36,** 9186–9200 (2016).

126. Devraj, K., Guérit, S., Macas, J. & Reiss, Y. An In Vivo Blood-brain Barrier Permeability Assay in Mice Using Fluorescently Labeled Tracers. *J. Vis. Exp.* (2018). doi:10.3791/57038